การประยุกต์ CIECAM02 กับภาพที่ไม่ทราบสีขาวอ้างอิง

นายมติ บุญเติม

APPLYING CIECAM02 TO IMAGES WITH UNKNOWN REFERENCE WHITE

Mr. Mati Bunterm

A Thesis Submitted in Partial Fulfillment of the Requirements

for the Degree of Master of Science in Imaging Technology

Department of Imaging and Printing Technology

Faculty of Science

Chulalongkorn University

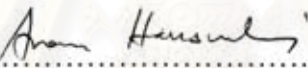Academic year 2005

ISBN 974-17-4243-6

Thesis Title   Applying CIECAM02 to Images with Unknown Reference White

By   Mr. Mati Bunterm

Field of study   Imaging Technology

Thesis Advisor   Suchitra Sueeprasan, Ph.D.

Thesis Co-advisor   Assistant Professor Pei-Li Sun, Ph.D.

Accepted by the Faculty of Science, Chulalongkorn University in Partial Fulfillment of the Requirements for the Master's Degree

....Dean of The Faculty of Science

(Professor Piamsak Menasveta, Ph.D.)

THESIS COMMITTEE

....Chairman

(Associate Professor Aran Hansuebsai, Ph.D.)

....Thesis Advisor

(Suchitra Sueeprasan, Ph.D.)

....Thesis Co-advisor

(Assistant Professor Pei-Li Sun, Ph.D.)

....Member

(Pichayada Katemake, Ph.D.)

มติ บุญเติม : การประยุกต์ CIECAM02 กับภาพที่ไม่ทราบสีขาวอ้างอิง
(APPLYING CIECAM02 TO IMAGES WITH UNKNOWN REFERENCE WHITE)
อ. ที่ปรึกษา : อ. ดร. สุจิตรา สื่อประสาร, อ.ที่ปรึกษาร่วม : ASST. PROF. PEI-LI SUN, Ph.D., 93
หน้า. ISBN 974-17-4243-6.

งานวิจัยนี้มีจุดมุ่งหมายที่จะประยุกต์แบบจำลองการปรากฏสี (CIECAM02) กับภาพที่ไม่ทราบสี
ขาวอ้างอิง ซึ่งค่าสีขาวอ้างอิงเป็นตัวแปรที่สำคัญตัวหนึ่งในการทำงานของแบบจำลองการปรากฏสี โดยการ
ใช้ค่าสีขาวอ้างอิงที่ผลิตได้จาก 4 ทฤษฎี คือ White Patch, Gray World, CIE Illuminant D65 และ การใช้
ค่าสีขาว (White point) ของจอภาพ มาเป็นค่าสีขาวอ้างอิงให้กับภาพที่ไม่ทราบค่าสีขาวอิง 3 รูป คือ Fruits,
Wine และ Orchids ทฤษฎีที่เหมาะสมกับการนำมาประยุกต์ใช้ จะต้องทำให้ภาพทดสอบที่ผลิตได้จาก
แบบจำลองการปรากฏสี CIECAM02 ที่ใช้ค่าสีขาวอ้างอิงตามทฤษฎีดังกล่าว มีสีใกล้เคียงกับภาพต้นฉบับ
มากที่สุด ซึ่งวัดโดยพิจารณาจากคะแนนความเหมือนที่ได้จากกลุ่มผู้สังเกต และจากผลการทดลองสามารถ
สรุปได้ดังนี้ คะแนนของค่าสีขาวอ้างอิงที่ได้จากทฤษฎี White Patch ค่อนข้างคงที่ในแต่ละภาพของ
ต้นฉบับ แต่คะแนนที่ได้ยังไม่อยู่ในเกณฑ์ที่ดีที่สุด คะแนนของทฤษฎี Gray world นั้นไม่คงที่ขึ้นอยู่กับ
ชนิดของภาพต้นฉบับ โดยมีคะแนนที่สูงกับภาพที่สีสวนใหญ่เป็นสีเทา (Wine) และได้คะแนนที่ต่ำกับภาพ
ที่มีสีสันมาก (Fruits) เช่นเดียวกันกับค่าสีขาวอ้างอิงที่มาจากค่ามาตรฐาน CIE Illuminant D65 ซึ่งได้
คะแนนที่ไม่คงที่ แตกต่างกันที่สีขาวอ้างอิง D65 นั้นให้ค่าที่ดีกับภาพที่มีสีสันมากเช่น Fruits แต่ได้คะแนน
ที่ยังไม่ดีกับภาพอื่น ๆ ส่วนสีขาวอ้างอิงที่มาจากค่าสีขาวของจอภาพนั้น ได้คะแนนที่อยู่ในเกณฑ์ที่ดีในทุก
ภาพของต้นฉบับ ซึ่งเมื่อพิจารณาจากผลโดยรวมแล้ว ทฤษฎีที่เหมาะสมสำหรับนำมาประยุกต์ใช้กับภาพที่
ไม่ทราบสีขาวอ้างอิง จึงเป็นค่าสีขาวอ้างอิงที่มาจากค่าสีขาว (White point) ของจอภาพ เนื่องจากผลที่ได้ใน
แต่ละภาพต้นฉบับอยู่ในเกณฑ์ที่ดีทั้งหมด

ภาควิชา วิทยาศาสตร์ทางภาพถ่ายและเทคโนโลยีทางการพิมพ์ ลายมือชื่อนิสิต.......................................
สาขาวิชา ....เทคโนโลยีทางภาพ...............ลายมือชื่ออาจารย์ที่ปรึกษา...............................
ปีการศึกษา ....2548....................... ลายมือชื่ออาจารย์ที่ปรึกษาร่วม...............................

The aim of this thesis was to investigate the means of applying CIECAM02 color appearance model to images with unknown reference whites. The investigation was done by estimating reference whites of digital images using four different models: white patch (WP), gray world (GW), the CIE illuminant D65 (D65) and the white point of the CRT monitor (CRT), which were tested to be used as the parameter in CIECAM02. There were three original images: "Fruits", "Wine", and "Orchids". Images reproduced via CIECAM02 with suitable reference whites would give good color matches to the original images. The result showed that there were not the reference-white estimation models that gave the best result in all cases. WP performed consistently for all images but it did not give a good result. GW gave good color matches for achromatic images such as "Wine" but did not work well for colorful images like "Fruits". D65 provided the best result for the colorful image but did not give a good result in other cases. Overall, the white point of the testing monitor (CRT) was recommended because its performance was less dependent on images and yielded a high accuracy in all cases.

Department Imaging and Printing Technology Student's Signature..

Field of study.........Imaging Technology........ Advisor's signature...

Academic year.............2005..................... Co-advisor's signature......................................

ACKNOWLEDGEMENTS

First and foremost, I wish to express my sincere appreciation to my advisor Dr. Suchitra Sueeprasan for her invaluable contribution to the improvement of this thesis and her kind supervision, invaluable guidance and suggestion throughout this study.

Thank you to everybody at the Department of Imaging and Printing Technology, Faculty of Science, Chulalongkorn University for their help. Special thanks for my friends at Rotaract Club of Chulalongkorn University for their suggestion and moral supports.

Last but not least, I wish to express my deep gratitude to by parent for their love, inspiration, understanding and their endless encouragement and supports throughout this entire study, thanks for giving my life.

CONTENTS

Page

List of Tables

List of Figures

CHAPTER I

INTRODUCTION

1.1 Backgrounds

At present, digital imaging technologies have been developed rapidly. The use of digital devices such as digital camera, displays prevails in many industries, including the graphic arts industry. CRT monitors are commonly used as soft proofing prior to printing. In a process of color image reproduction, a digital camera is becoming an important input device due to its expediency. An image captured with digital cameras is readily digitized and viewed on a monitor. The image displayed on the monitor is normally edited before transferring to other stages in the process. When viewing the image under different viewing condition, its color appearance usually differs. The perception of color by the human visual system is different from the sensitivity of digital devices' sensors. Human sensation of color is the processing of light energy first by eye and later by the brain. The human visual system perceives colors according to viewing conditions under which images are viewed. A visual mechanism called chromatic adaptation is active to discount the color of light source used to illuminate the images. On the other hand, sensors of digital devices response to the total amount of light energy. For example, a picture of white paper taken under a yellowish light will look more yellowish than the real scene seen by eyes. This is because the chromatic adaptation mechanism

takes place; therefore, the color of the light source is removed from the scene, preserving the perception of white paper. In contrast, the picture from digital cameras is the result of the light reflected from the paper, which has more energy in long wavelength (yellowish) due to the effect of light source. Thus, to achieve successful color image reproduction, a color appearance model capable of predicting color appearance under various viewing conditions is needed. An image is transferred from one stage to another in the process of color reproduction with the color appearance match throughout the process due to the use of color appearance model. In 1997, the International Commission on Illumination (CIE), developed the color appearance model namely CIECAM97s[1] for general use. In 2002, CIECAM02 was proposed to replace CIECAM97s. The CIECAM02 is based on CIECAM97s but predicts more correctly chroma and saturation.[2,3]

The CIECAM02 is able to predict the appearance of colors under different viewing conditions. In so doing, it requires input parameters associated with viewing conditions: surround, background, luminance of adapting field and a reference white. The reference white of the scene is the key to correctly predicting the color appearance. This is because the reference white represents the color of light source illuminating the scene. When images are hardcopies or in digital form with known viewing conditions, the CIECAM02 can be applied without any difficulty. However, when an image from a digital camera is used, the viewing conditions under which the image was taken is usually unknown, resulting in an unknown reference white for the image. In order to apply

CIECAM02 successfully, the reference white needs to be estimated from the image. The correctly estimated reference white applied to CIECAM02 will provide a good color match when transferred to different viewing conditions. There are a number of ways to estimate reference whites from images, for example, Gray world[4,5], Modified gray world[6], White patch retinex[7,8]. Alternatively, the standard reference whites such as CIE illuminant D50 or CIE illuminant D65 can also be applied directly. This study thus investigated the way to successfully apply CIECAM02 to images having no pre-defined reference white for use in the process of color image reproduction. Four methods of estimating reference white: Gray world, White pate, CIE illuminant D65 and the white point of the monitor were tested to determine which method could be best applied to CIECAM02 in order to produce good color matches for images with unknown reference white.

1.2 Objective

To investigate the accuracy of methods of reference-white estimation as to accommodate the applications of CIECAM02 in color image reproduction, which involve an image with unknown reference white.

1.3 Scope of research

Four methods of estimating reference white: White patch (WP), Gray world (GW), CIE illuminant D65 (D65) and the white point of the monitor (CRT), were tested in this study. Three digital images with different scene

contents were perturbed with yellow and then used as originals. CIECAM02 was applied to produce color appearance matches to the originals under an equal energy white (S_E) condition. A series of originals and reproduction images was shown on a CRT monitor in a darkened room. Visual experiments were conducted to identify best color matches by means of the category judgment and the memory matching techniques. Fifteen observers with normal color vision took part in the experiment.

1.4 Expected outcomes

An appropriately accurate method of reference-white estimation with respect to the use of CIECAM02 for images with unknown reference white.

1.5 Contents of the thesis

This chapter discusses the backgrounds, objective, expected outcome, as well as the scope of this study. In Chapter II, the theory and literature reviews of this research are described. The experimental set-up is explained in Chapter III. Chapter IV provides details of experimental results together with their discussions, which are followed by conclusions and suggestion of the thesis in Chapter V.

CHAPTER II

THEORY AND LITERATURE REVIEW

2.1 Theory

This thesis concerns the application of CIECAM02 for digital images having no information on their reference whites. To fully understand the aim of this study and how the experiment had been set up, some basic theories need to be addressed. These include the perception of color (Section 2.1.1), the CIE color system (Section 2.1.2), some color-appearance phenomena (Section 2.1.3), viewing condition (Section 2.1.4), chromatic adaptation (Section 2.1.5), color appearance model (Section 2.1.6), methods of estimating reference whites (Section 2.1.7), and psychophysics (Section 2.1.8).

2.1.1 The perception of color [9,10]

Color perception involves three basic factors, i.e. the source of light, objects under illumination, and the eyes and neural responses of observers. The visual process begins when radiant energy from the source strikes the object and some of this energy is reflected and passes through the lens to strike the retina in the eye. The retina is made up of a complex network of cells and neurons. The retina consists of a large number of cells which are sensitive to light; these receptors cells are of two kinds, rods and cones. Rods are sensitive

to brightness of light only at low illuminate. Cones are cells of three different types, which respond to red, blue and green regions of light, respectively, and it is through these that all colors are seen. When the three types of cones are all stimulated equally, the eye and the brain see achromatic, but if one type of cone is stimulated more than the other two, the image appears to be tinted with the corresponding primary hue.

The most central part of the retina is called the fovea and it has the largest concentration of cells. The fovea vision is used for distinguishing very fine detail such as reading and seeing objects at distance. Outside the fovea, the number of cones is greatly reduced and they are situated quite apart from one another. The rods are completely absent from the fovea and fall out to the extreme periphery. The signals leave the retina via the optic nerve and eventually arrive at back of the brain. The brain signals are interpreted through mental impressions that result in perception.

2.1.2 The CIE color system

The CIE colorimetric system comprises the essential standards and procedures of measurement that are necessary to make colorimetry a useful tool in science and technology. The CIE system is usually employed in connection with instruments for color measurement. This system has been established by the Commission Internationale de I' Eclairage, the French title of international committee, or International Commission of Illumination in 1931. The CIE system started with the premise developed on the human color

perception process that stimulus for color is provided by the proper combination of a source of light and on observer [11].

2.1.2.1 Calculation of tristimulus values from spectral data[12,13]

Trisimulus values are calculated from the emitted spectrum of an object, a CIE standard illuminant, and one of the CIE standard observers. The CIE tristimulus values X, Y and Z of a color are obtained by multiplying together the relative power S_λ of a CIE standard illuminant, the reflectance factor R_λ of the object and the standard observer functions $\bar{x}_\lambda, \bar{y}_\lambda, \bar{z}_\lambda$. The products are summed up for all the wavelengths in the visible spectrum, and then their sums are normalized, resulting in the CIE tristimulus values. The corresponding mathematical equations shown as follows:

$$X = k \sum_\lambda S_\lambda R_\lambda \bar{x} \Delta\lambda \qquad (2.1)$$

$$Y = k \sum_\lambda S_\lambda R_\lambda \bar{y} \Delta\lambda \qquad (2.2)$$

$$Z = k \sum_\lambda S_\lambda R_\lambda \bar{z} \Delta\lambda \qquad (2.3)$$

$$k = \frac{100}{\sum_\lambda S_\lambda R_\lambda \bar{y} \Delta\lambda} \qquad (2.4)$$

where S_λ is a CIE illuminant, R_λ is the object's spectral reflectance factor, $\bar{x}_\lambda, \bar{y}_\lambda$ and $\bar{z}_\lambda$ are the CIE standard observer color-matching functions, $\sum_\lambda$ represents summation across wavelength, k is a normalizing constant, and

$\Delta\lambda$ is the measurement wavelength interval (for objects it is usually either 10 or 20 mm. By definition, CIE color-matching functions are defined from 360 nm to 780 nm in 10 nm.

2.1.3 Color appearance phenomena

Two stimuli with identical CIE XYZ trisimulus values will match in color for an average observer as long as certain constraints are followed[14]. These constraints include the retinal focus of stimulation, the angular subtense, and the luminance level. In addition, the two stimuli must be viewed with identical surrounds, backgrounds, size, shape, surface characteristics, illumination geometry, and etc. If any of these constraints are violated, it is likely that the color match will no longer hold. However, in many practical applications, the constraints necessary for successful color match prediction using simple tristimulus colorimetry can not be met. It is these applications that require colorimetry to be enhanced to include the influences of these variables. Such enhancements are color appearance models. The various phenomena that "break" the simple XYZ tristimulus system are the topics of the following sections. Fig. 2.1 illustrates a simple example of one color-appearance phenomenon: simultaneous contrast, or induction. In Fig. 2.1 (a), the two gray patches with identical XYZ trisimulus values match in color because they are viewed under identical conditions (both on the same gray background). If one of the gray patches is placed on a white background and the other on a black background, as in Fig. 2.1 (b), the two patches no longer match in appearance.

Their tristimulus values, however, remain equal. Since the constraint that the stimulus is viewed in identical conditions is violated in Fig. 2.1 (b), tristimulus colorimetry can no longer predict a match. Instead, a model that includes the effect of background luminance factor on the appearance of the patches would be required.
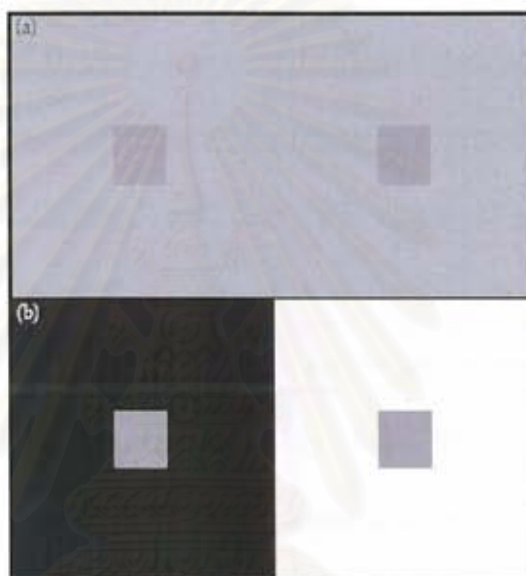
Fig. 2.1 An example of simultaneous contrast. The gray patches on the gray background (a) are physically identical to those on the white and black backgrounds (b). [15]

There are many color-appearance that affect changes of color appearance due to changes of viewing condition. These phenomena justify the need to develop color appearance models and define the required input data and output predictions. Some of the phenomena are discussed in the following sections.

2.1.3.1 Simultaneous contrast

Fig. 2.1 illustrates simultaneous contrast, as previously described. The two identical gray patches presented on different backgrounds appear distinct. The black background causes the gray patch to appear lighter, while the white background causes the gray patch to appear darker. Simultaneous contrast causes a stimulus to shift in color appearance when the color of its background is changed. These apparent color shifts follow the opponent-colors theory of color vision in a contrasting sense along the opponent dimensions. In other words, a light background induces a stimulus to appear darker, a dark background induces a lighter appearance, red induce green, green induces red, yellow induces blue, and blue induce yellow. Josef Albers[16], in his classis study Interaction of Color, explored various aspects of simultaneous contrast and taught artists and designers how to avoid the pitfalls and take advantage of the effects. More-complete explorations of the effect are available in classic color-vision texts such as Hurvich[17], Boynton[18], and Evans[19]. Cornelissen and Brenner[20] explored the relationship between adaptation and chromatic induction based on the concept that induction can be at least partially explained by localized chromatic adaptation. Blackwell and Buchsbaum[21] described some of the spatial and chromatic factors that influence the degree of induction.

Robertson[22] presented an interesting example, reproduced in Fig. 2.2, of chromatic induction that highlights the complex spatial nature of this phenomenon. The red squares in Fig. 2.2 (a) or the cyan squares in Fig. 2.2 (b),

are all surrounded by the same chromatic edges (two yellow edges and two blue edges for each square). If chromatic induction were strictly determined by the colors at the edges, then all of the red squares and all of the cyan squares should appear similar. However, it is clear from Fig. 2.2 that the squares that appear to be falling on the yellow stripes are subject to induction from the yellow and thus appear darker and bluer. On the other hand, the squares falling on the blue stripes appear lighter and yellower. Clearly, the simultaneous contrast for these stimuli depends more on the spatial structure than simply the local edges.

(a)   (b)

Fig. 2.2 Stimuli patterns that illustrate the complexity of simultaneous contrast.[22]

The local contrasts for the left and right sets of squares are identical. However, simultaneous contrast is apparently driven by the stripes on which the square patches appear to rest.

2.1.3.2 Hunt Effect (Colorfulness increases with luminance)

The Hunt effect obtains its name from a study of the effects of light and dark adaptation on color perception published by Hunt[23]. In that study, Hunt

collected corresponding colors data via haploscopic matching, in which each eye was adapted to different viewing conditions and matches were made between stimuli presented in each eye. Fig. 2.3 shows a schematic representation of Hunt's results. The data points represent corresponding colors for various level of adaptation. What these results show is that stimulus of low colorimetric purity viewed at 10,000 cd/m^2 is required to match a stimulus of high colorimetric purity viewed at 1 cd/m^2. Stated more directly, as the luminance of a given color stimulus is increased, its perceived colorfulness also increases.
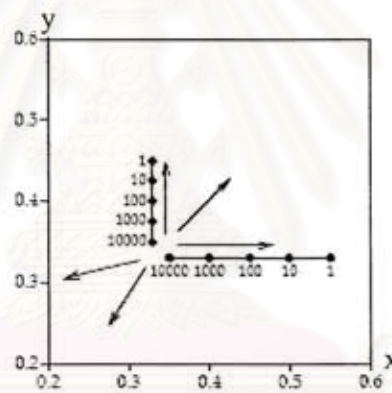
Fig. 2.3 A schematic representation of corresponding chromaticities across changes in luminance showing the Hunt effect. Points are labeled with luminance levels.[15]

2.1.3.3 Stevens effect (contrast increase with luminance)

The Stevens effect is a close relative of the Hunt effect. While the Hunt effect refers to an increase in chromatic contrast (colorfulness) with luminance, the Stevens effect refers to an increase in brightness (or lightness) contrast with

in creasing luminance. For the purposes of understanding these effect, contrast should be thought of as the rate of change of perceived brightness (or lightness) with respect to luminance.

Like the Hunt effect, the Steven effect draws its name from a classic psychophysical study (Stevens and Stevens[24]). In this study, observers were asked to perform magnitude estimations on the brightness of stimuli across various adapting conditions. The results illustrated that the relationship between perceived brightness and measured luminance tended to follow a power function. This power function is sometimes called, in psychophysics, the Stevens Power law. A relationship that follows a power function when plotted on linear coordinates becomes a straight line (with slope equal to the exponent of the power function) on log-log coordinates. Typical results from Stevens and Stevens[24] experiments are plotted on logarithmic axes in Fig. 2.4. That figure shows average relative brightness magnitude estimations as a function of relative luminance for four different adaptation levels. The figure shows that the slope of this relationship (and thus the exponent of the power function) increases with increasing adaptation luminance.

The Stevens effect indicates that as the luminance level increases, dark colors will appear darker and light colors will appear lighter. While this prediction might seem somewhat counterintuitive, it is indeed the case. The Stevens effect can be demonstrated by viewing an image at high and low luminance levels. A black-and-white image is particularly effective for this demonstration. At a low luminance level, the image will appear to have rather

low contrast. White areas will not appear very bright and, perhaps surprisingly, dark areas will not appear very dark. If the image is then moved to a significantly higher level of illumination, white areas appear substantially brighter and dark areas appear darker - the perceived contrast has increased.
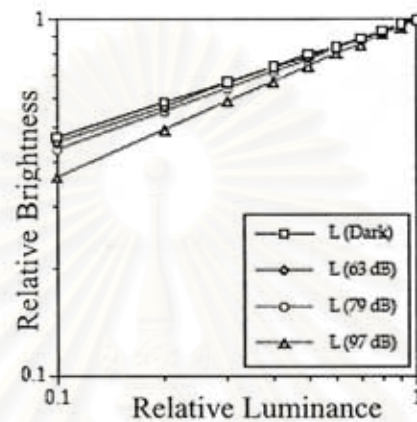
Fig. 2.4 Changes in lightness contrast as a function of adapting luminance according to the Stevens effect.[15]

From Steven and Hunt effect, when the luminance level was increasing the scene will appear more contrast and more colorfulness. Fig. 2.5 shown the images that has different luminance level.
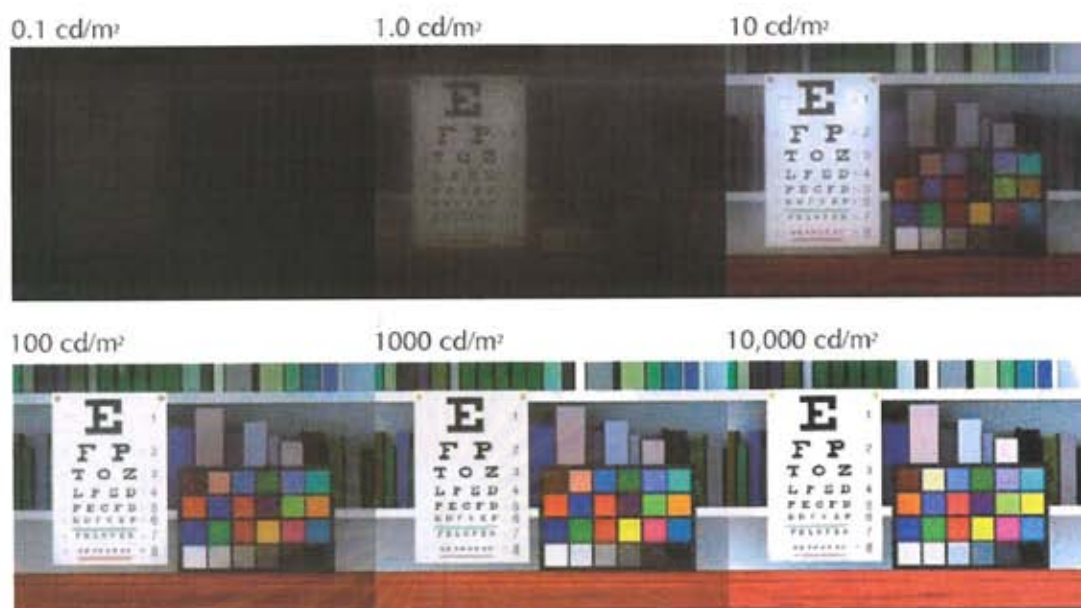
Fig. 2.5 The images that were shown in difference luminance level.[15]

2.1.4 Viewing Condition

Some of the various color appearance phenomena that produce the need for extensions to basic colorimetry were presented in the previous sections. It is clear from these phenomena that various aspects of the visual field impact the color appearance of stimulus. Different configurations of the viewing field will result in different cognitive interpretations of a stimulus and, in turn, different color perceptions. There are various definitions of standard viewing conditions used in different industries. These attempt to minimize difficulties with color appearance by defining appropriate viewing field configurations.

2.1.4.1 Configuration of the Viewing Field

The color appearance of stimulus depends on the stimulus itself as well as on other stimuli that are nearby in either space of time. Temporal effects, while important, are generally not encountered in typical color-appearance applications. They are dealt with by ensuring that observers have had adequate time to adapt to the viewing environment and presenting stimuli that do not vary in time. (However, there are several recent applications, such as digital video, that will push color-appearance studies toward the domain of temporal variation.) The spatial configuration of the viewing field is a way of critical importance. (Since the eyes are constantly in motion, it is impossible, in practical situations, to separate spatial and temporal effects.) The ideal spatial representation of the visual field would be to have a fully specified image of the scene. Such an image would have to have a spatial resolution greater than the visual acuity of the fovea and each pixel would be represented by a complete spectral power distribution. With such a representation of the entire visual field, one would have almost all of the information necessary to specify the color appearance of any element of the scene; however, the cognitive experience of the observer and temporal information would still be missing. Some interesting recent data on the impact of the spatial configuration of stimulus and surround were published by Abramov et al.[25]

Such a specification of the viewing field is not practical for several reasons. First, the extensive data required are difficult to obtained accurately, even in a laboratory setting. It is not plausible to require such data in practical

applications. Second, even if the data could be obtained, its huge volume would make its use quite difficult. Third, assuming these technical issues were overcome, one would then require a color appearance model capable of utilizing all of that data. Such a model does not exist and is not likely to be developed in the foreseeable future. When the inter-observer variability in color-appearance judgments is considered, such a detailed model would certainly be unnecessarily complex.

Given these limitations, the situation is simplified by defining a minimum number of important components of the viewing field. The various color appearance models use different subsets of these viewing-field components. The most extensive set is the one presented by Hunt[26,27] for use with his color appearance model. Since Hunt's definition of the viewing field includes a superset of the components required by all other models, his definitions are presented in four components:

1. Stimulus
2. Proximal field
3. Background
4. Surround
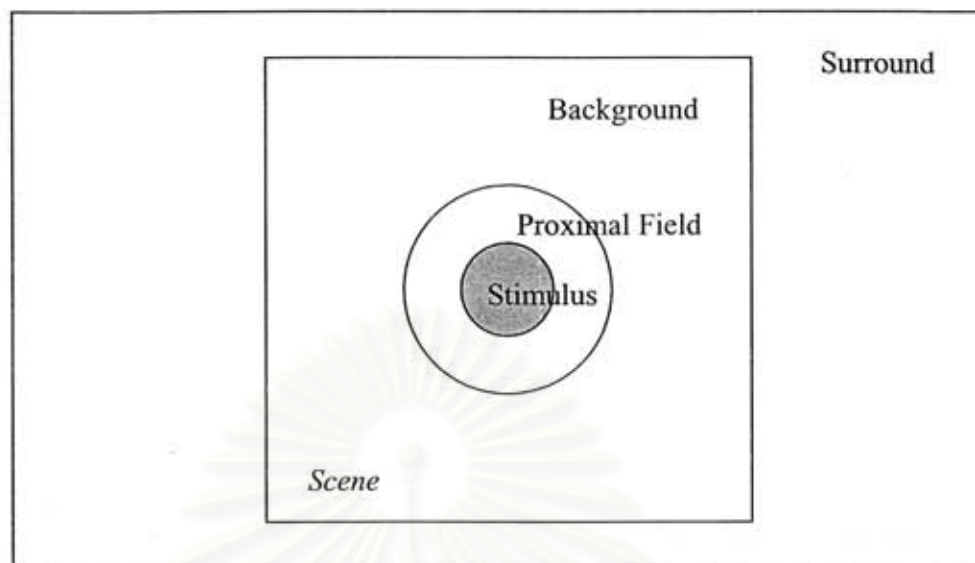
Fig. 2.6 Schematically represents these components of the visual field.

Stimulus

Stimulus is the color element for which a measure of color appearance is desired. Typically the stimulus is taken to be a uniform patch of about 2 degree angular subtense. A stimulus of approximately 2° subtense is assumed to correspond to the visual field appropriate for use of the CIE 1931 standard colorimetric observer. The 1931 observer is considered valid for stimuli ranging from 1 degree to 4 degree in angular subtense[28]. Trichromatic vision breaks down for substantially smaller stimuli. The CIE 1964 supplementary standard colorimetric observer should be considered for use with large stimuli (10° or greater angular subtense).

When viewing real scenes, observers often consider an entire object as "uniform" stimulus. For example, one might ask, what color is that car? Even

though different areas of the car will produce widely different color appearances, most observers would reply with a single answer. Thus the stimulus is not a 2° field, but rather the entire object. This occurs to a limited extent in images. However, it is more conceivable for observers to break an image apart into smaller image elements.

Proximal Field

A proximal field is the immediate environment of the stimulus extending for about 2° from the edge of the stimulus in all, or most, directions. The definition of the proximal field is useful for modeling local contrast effects such as lightness of chromatic induction.

Background

The background is defined as the environment of the stimulus, extending for about 10° from the edge of the stimulus (or proximal field, if defined) in all, or most, directions. Specification of the background is absolutely necessary for modeling simultaneous contrast. If the proximal field is different, its specification can be used for more complex modeling.

As with the proximal field, defining the background in imaging applications is difficult. For given image element, the background usually consists of the surrounding image areas, the exact specification of which will change with image content and by location in the image. Thus precise

specification of the background in images would require point-wise recalculation of appearance-model parameters. Since this is impractical in any typical applications, the background is usually assumed to be constant and of some medium chromaticity and luminance factor (e.g., a neutral gray with 20% luminance factor).

Surround

A surround is the field outside the background. In practical situations, the surround can be considered to be the entire room or the environment in which the image (or other stimulus) is viewed. For example, print images are usually viewed in an illuminated (average) surround, projected slides in a dark surround, and video displays in a dim surround. Thus, even in imaging applications, it is easy to specify the surround. It is the area outside the image display filling the rest of the visual field.

Specification of the surround is important for modeling induction, flare (stimulus and within the eye), and overall image contrast effects. Practical difficulties arise in specifying the surround precisely when typical situations are encountered, particularly those involving a wide range of surround relative luminances and inhomogeneous spatial configurations.

2.1.5 Chormatic Adaptation

Chromatic adaptation is the human visual system's capability to adjust to widely varying colors of illumination in order to approximately preserves the appearance of object colors[14]. Chromatic adaptation is the largely independent sensitivity regulation of the mechanisms of color vision. Often it is considered to be only the independent changes in responsivity of the three types of cone photoreceptors. However, it is important to keep in mind that there are other mechanisms of color vision (e.g., at the opponent level and even at the object recognition level) that are capable of changes in sensitivity that can be considered mechanisms of chromatic adaptation.

To see an example of chromatic adaptation, consider a piece of white paper illuminated by daylight. When the paper is in a room with incandescent light, it still appears white despite the fact that the energy reflected from the paper has changed from predominantly blue to predominantly yellow. Fig. 2.7 shows the example of chromatic adaptation; Fig. 2.7 (a) is the original image. Fig. 2.7 (b) is the image that was made by using green filter. And Fig. 2.7 (c) is the image that only banana was green by using the same filter of Fig. 2.7 (b). The effect of chromatic adaptation was found in the banana of Fig. 2.7 (b) and Fig. 2.7 (c), the banana looks like different colors but they are the same stimuli.
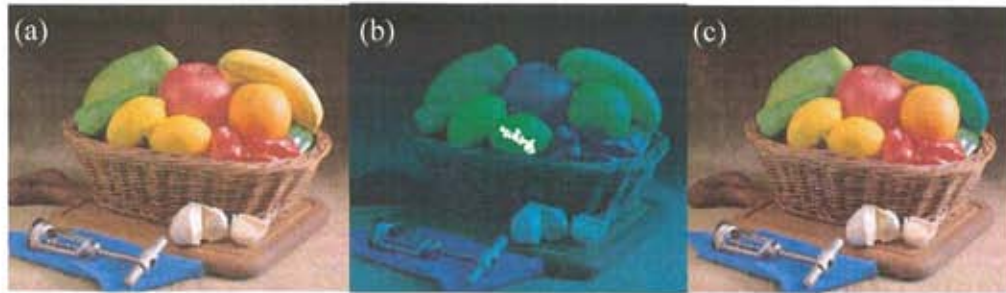
Fig. 2.7 The example of chromatic adaptation; (a) is the original image, (b) is the image that was used green filter and (c) is the image that was used the same filter of (b) only in banana.[15]

2.1.6 Color appearance model

A color appearance model tries to model how the human visual system perceives colors of an object under different lighting conditions and with different backgrounds. It aims to make a mathematical link between the basic colorimetry of light sources, materials and the viewing environment and the apparent color of a given stimulus in that environment, as described by its color appearance attributes. An image that is viewed under one lighting condition can be adjusted to appear to have the same colors if it were viewed under a completely different lighting condition. The ability of a color appearance model to perform this task means that it can be used to develop a device-independent way of storing images. For example, if an image is scanned into a computer, the color appearance model, knowing the scanner's illumination conditions, can transform the image into its internal representation. When the image would be displayed on a monitor or printed, again the color appearance,

knowing the output display's illumination conditions, can transform its internal representation on the image to the correct representation for the output display[29].

For example, Fig. 2.8 (a) is one of color appearance phenomena, simultaneous contrast, a gray patch on the black background looks lighter than a gray patch on the white background but they are actually the same color patches. Fig. 2.8 (b) the patch on the white background was predicted by CIECAM02 color appearance model[30] and looks more like the patch on the black background than Fig. 2.8 (a).
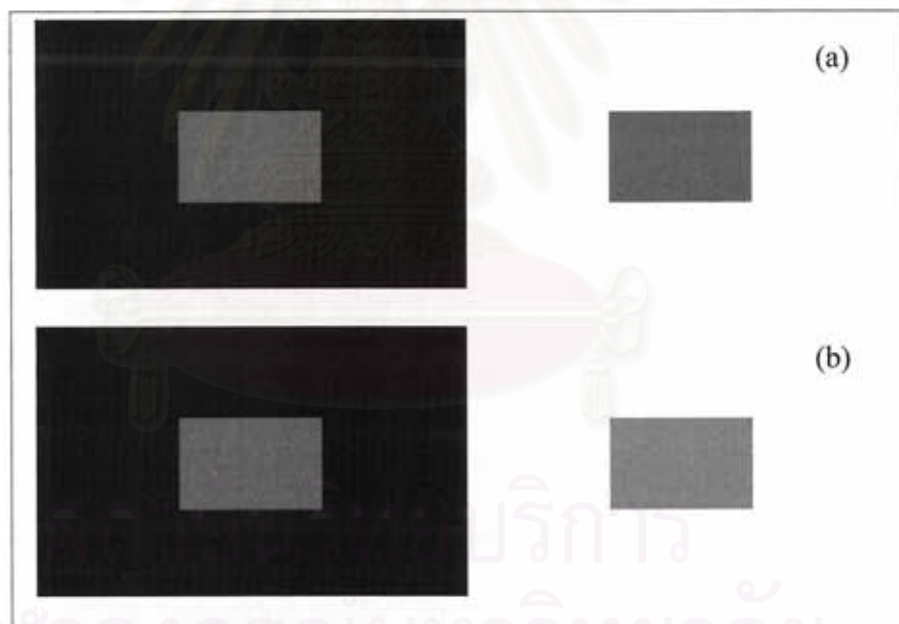
Fig. 2.8 The example of using color appearance model; (a) is the same color patch that was placed on different backgrounds, (b) is the patch that was predicted from CIECAM02 (right patch) to make two patches look the same on different backgrounds.[30]

2.1.6.1 The CIECAM02 color appearance model

The CIECAM02 color appearance model builds upon the basic structure and form of the CIECAM97s color appcarance model.[1] It provides a viewing condition specific means for transforming tristimulus values to or from perceptual attribute correlates. The two major pieces of this model are a chromatic adaptation transform and equations for computing correlates of perceptual attributes, such as brightness, lightness, chroma, saturation, colorfulness and hue. The chromatic adaptation transform takes into account changes in the chromaticity of the adopted white point. In addition, the luminance of the adopted white point can influence the degree to which an observer adapts to that white point. The degree of adaptation or D factor is therefore another aspect of the chromatic adaptation transform. Generally, between the chromatic adaptation transform and computing perceptual attributes correlates there is also a non-linear response compression. The chromatic adaptation transform and D factor was derived based on experimental data. The non-linear response compression was derived based on physiological data and other considerations. The perceptual attribute correlates were derived by comparing predictions to magnitude estimation experiments, such as various phases of the LUTCHI data[31], and other data sets, such as the Munsell Book of Color. Finally the entire structure of the model is generally constrained to be invertible in closed form and to take into account a sub-set of color appearance phenomena.[2]

Steps for calculate CIECAM02 forward model

Step 1 Set the viewing condition parameter of CIECAM02

It is convenient to begin by computing viewing condition dependent
constants. First the surround is selected and then values for F, c and Nc can be
read from Table 2.1.

Table 2.1 Viewing condition parameters for different surrounds

Surround	F	c	N_C
Average	1.0	0.69	1.0
Dim	0.9	0.59	0.95
Dark	0.8	0.52	0.8

The value of F_L can be computed using Equations 2.1 and 2.2, where L_A
is the luminance of the adapting field in cd/m^2.

$$k = \frac{1}{5L_A + 1} \tag{2.5}$$

$$F_L = 0.2k^4(5L_A) + .01(1-k^4)(5L_A)^{1/3} \tag{2.6}$$

The value n is a function of the luminance factor of the background and
provides a very limited model of spatial color appearance. The value of n
ranges from 0 for a background luminance factor of zero to 1 for a background
luminance factor equal to the luminance factor of the adopted white point. The
n value can then be used to compute N_{bb}, N_{cb} and z, which are then used during
the computation of several of the perceptual attribute correlates. These
calculations can be performed once for a given viewing condition.

$$n = \frac{Y_b}{Y_w} \tag{2.7}$$

$$N_{bb} = N_{cb} = 0.725 \left(\frac{1}{n}\right)^{0.2} \tag{2.8}$$

$$z = 1.48 + \sqrt{n} \tag{2.9}$$

Step 2 Compute the chromatic adaptation

Once the viewing condition parameters have been computed, input tristimulus values can be processed. The processing begins with the chromatic adaptation transform. This transform consists of three major components. First is the space in which the transform is applied. Second is the specific transform and third is a model of incomplete adaptation.

The tristimulus values (XYZ) are transformed to CAT02 space (RGB) by using the equation below.

$$\begin{bmatrix} R \\ G \\ B \end{bmatrix} = M_{CAT02} \begin{bmatrix} X \\ Y \\ Z \end{bmatrix} \tag{2.10}$$

$$M_{CAT02} = \begin{bmatrix} 0.7328 & 0.4296 & -0.1624 \\ -0.7036 & 1.6975 & 0.0061 \\ 0.0030 & 0.0136 & 0.9834 \end{bmatrix} \tag{2.11}$$

The D factor or degree of adaptation is a function of the surround and L_A and in theory could range from 0 for no adaptation to the adopted white point to 1 for complete adaptation to the adopted white point. The D factor is computed by using Equation 2.12.

$$D = F\left[1 - \left(\frac{1}{3.6}\right)e^{\left(\frac{-L_A - 42}{92}\right)}\right] \tag{2.12}$$

Given the D factor and data transformed using M_{CAT02}, the full chromatic adaptation transform can be written:

$$R_C = \left[\left(\frac{Y_w D_w}{R_w}\right) + (1 - D)\right]R \tag{2.13}$$

Where the w subscript denotes the corresponding value for the white point and the c subscript denotes stimuli values. G_c and B_c can be calculated in a similar manner, as can R_{cw}, G_{cw} and B_{cw}. Equation 2.13 includes the factor Y_w in the calculation so that the adaptation is independent of the luminance factor of the adopted white point.

The R_c, G_c and B_c values are then converted to Hunt-Pointer-Estevez space[32] by using Equation 2.14 before the post-adaptation nonlinear response compression is applied.

$$\begin{bmatrix} R' \\ G' \\ B' \end{bmatrix} = M_H M_{CAT02}^{-1} \begin{bmatrix} R_C \\ G_C \\ B_C \end{bmatrix} \tag{2.14}$$

$$M_H = \begin{bmatrix} 0.38971 & 0.68898 & -0.07868 \\ -0.22981 & 1.18340 & 0.04641 \\ 0.00000 & 0.00000 & 1.00000 \end{bmatrix} \tag{2.15}$$

$$M_{CAT02}^{-1} = \begin{bmatrix} 1.096124 & -0.278869 & 0.182745 \\ 0.454369 & 0.473533 & 0.072098 \\ -0.009628 & -0.005698 & 1.015326 \end{bmatrix} \tag{2.16}$$

And the last step for achromatic adaptation, the post-adaptation non-linear response compression is then applied to the output from Equation 10. This function is based on a generalized Michaelis-Menten equation[33] and is consistent with Valeton and van Norren's physiologically derived data[34].

$$R'_a = \frac{400(F_L R'/100)^{0.42}}{[27.13 + (F_L R'/100)^{0.42}]} + 0.1 \qquad (2.17)$$

Step 3 Compute the perceptual attribute correlates

Preliminary Cartesian coordinates (a, b) are computed from the output from Equation 2.17. These values are used, in turn, to compute a preliminary magnitude t.

$$a = R'_a - \frac{12G'_a}{11} + \frac{B'_a}{11} \qquad (2.18)$$

$$b = (1/9)(R'_a + G'_a - 2B'_a) \qquad (2.19)$$

$$t = \frac{e(a^2 + b^2)^{1/2}}{(R'_a + G'_a + (21/20)B'_a)} \qquad (2.20)$$

A hue angle (h) is computed and this angle is also used to compute an eccentricity factor, e. This eccentricity value ranges from 0.8 to 1.2 as a function of the value of h.

$$h = \tan^{-1}(b/a) \qquad (2.21)$$

$$e = \left(\frac{12500}{13} N_c N_{cb}\right)\left[\cos\left(h\frac{\pi}{180} + 2\right) + 3.8\right] \qquad (2.22)$$

The achromatic response (A) can then be computed, as can be seen in Equation 2.23 and the value for lightness (J) is computed using the same equation as for CIECAM97s.

$$A = [2R'_a + G'_a + (1/20)B'_a - 0.305]N_{bb} \qquad (2.23)$$

$$J = 100(A/A_W)^{cz} \qquad (2.24)$$

Given lightness and the temporary magnitude, t, the value for chroma can then be computed as shown in Equation 2.25.

$$C = t^{0.9}\sqrt{J/100}(1.64 - 0.29^n)^{0.73} \qquad (2.25)$$

Finally, the tristimulus values (X, Y, Z) are transformed to CIECAM02 color space that have three major values, lightness (J), Chroma (C) and hue (h). The data output from CIECAM02 forward model (J, C, h) can be used for predicting the colors in other environments via CIECAM02 inverse model with appropriate viewing parameters of the second environment. The equations of CIECAM02 inverse model are given in Appendix A.

2.1.7 Reference white estimation

When digital images are taken under unknown light sources, one form of reference white estimations is applied in order to process the images into further stages such as color correction. Two methods of reference white estimations used in this study are described below.

Gray world

The chromaticity of the illuminant is determined from the average of all the pixels in an image. Gray world assumes that the average color of the scene is gray and that any departure from this average in the image is caused by the color of the illuminant. The performance of this method will be poor when the test images have different average distributions from the ones used for computing the database average.[5]

White patch

The white patch algorithm determines white from the maximum R, maximum G and maximum B found in the image, and hence the illuminant color. This algorithm has roots in the family of retinex algorithms, but it is only equivalent to it under restricted circumstances.[8]

2.1.8 Psychophysics

A scientific method of finding a relationship between physical stimuli intensity and human perception is called psychophysics. This study conducted visual experiments to identify a good performing method of estimating reference white using some forms of psychophysics. They were the memory viewing and category judgment techniques, which are described below.

2.1.8.1 Memory viewing technique

In the memory viewing technique[35], the original images and the reproduction images cannot be viewed at the same time. It is a technique that allows observers to fully adapt to a particular viewing condition. Observers have to adapt to an initial set of conditions for at least 1 minute in order to reach the steady state of adaptation before viewing images under these conditions. After memorizing the images, observers adapt to the second viewing conditions for at least 1 minute, the view the reproductions under the second conditions without viewing the original again.

2.1.8.2 Category judgment[36]

This scaling method is based on Torgerson's Law of Categorical Judgment[37]. The law of categorical judgments may be expressed mathematically as

$$B_k - R_j = z_{ij}\left(\sigma_j^2 + \sigma_k^2 - 2r_{jk}\sigma_j\sigma_k\right)^{\frac{1}{2}} \qquad (2.26)$$

where

B_k = the mean location of the kth category boundary,

R_j = the mean response to stimulus j,

σ_j = the dispersion of the kth category boundary,

σ_k = the dispersion of stimulus j,

r_{jk} = the correlation between momentary positions of stimulus k and category boundary k on the scale,

z_{jk} = the normal deviate corresponding to the proportion of times stimulus j is placed below boundary k.

Equation 2.26 represents the complete law of categorical judgments. Thurstone[38] stated five cases for that law, and Mosteller[39] has since added a sixth case. Each of these cases invokes certain assumptions, and the form of expression for scale values varies for simplifying assumptions. Table 2.2 sets forth the expressions for the six cases. Case I assumes replications over the judgments of one observer. For Case II, replications are over observers. In both cases the expression is the same as in Equation 2.26. Case III makes the simplifying assumption that the discriminal processes are independent, and thus their correlations are zero. Case IV assumes that, in addition, the discriminal dispersions are nearly equal, whereas Case V assumes that they are actually equal. Case Va relaxes the assumption of Case V in that the correlation of the discriminal processes may simply be constant rather than zero. It is common practice to set the scale unit equal to $\sigma(2)^{1/2}$ In Case V and equal to $\sigma(2[1-r_{ij}])^{1/2}$ in Case Va, so that the scale unit is simply equal to z_{ij} in both cases.

Table 2.2 Cases of the law of category judgment

Case	σ Constraints	r Constraints	Expression
I	σ_i unrelated to σ_j	$0 < r_{ij} \leq 1$	Equation (2.26)
II	σ_i unrelated to σ_j	$0 < r_{ij} \leq 1$	Equation (2.26)
III	σ_i unrelated to σ_j	$r_{ij} = 0$	$B_k - R_j = z_{ij}\left(\sigma_j^2 + \sigma_k^2\right)^{\frac{1}{2}}$
IV	$\sigma_i \cong \sigma_j$	$r_{ij} = 0$	$B_k - R_j = \left(2^{1/2}/2\right)z_{ij}\left(\sigma_j^2 + \sigma_k^2\right)^{\frac{1}{2}}$
V	$\sigma_i = \sigma_j$	$r_{ij} = 0$	$B_k - R_j = z_{ij}(2)^{\frac{1}{2}}$
Va	$\sigma_i = \sigma_j$	$r_{ij} = k$	$B_k - R_j = z_{ij}\left(2[1-r_{ij}]\right)^{\frac{1}{2}}$

In practice, we seldom know the values of σ and r (although they can be estimated). Instead, experimenters assume one of the cases. Occasionally, Case III is assumed to apply, but more often Case V or Va is used so that the scale values are simply values of z. In practice, then, we usually need only to determine the proportion of times one stimulus is preferred over another and calculate the standard normal deviate corresponding to that proportion to determine the interval-scale value of a stimulus. This can be done by comparing each stimulus with every other stimulus in turn to decide which stimulus shows more of the attribute under study. The steps for calculating the category judgment are given in Appendix B.

2.2 Literature review

Moroney et al.[2] described the newly proposed of color appearance model, called CIECAM02, which is based on CIECAM97s but included many revisions and some simplifications. A partial list of revisions includes a linear chromatic adaptation transform, a new non-linear response compression

function and modifications to the calculation for the perceptual attribute correlates. The forward equations of the CIECAM02 are also given in his paper. Li et al.[3] showed the three major drawbacks of the CIECAM97s model, and how the new model performed in various color regions. Both CIECAM97s and CIECAM02 models were tested using available data groups and the results are consistent in that CIECAM02 performed as well as, or better than, CIECAM07s in almost all cases. There was a large improvement in the prediction of saturation. In addition, CIECAM02 model can be considered as a possible replacement for CIECM97s for all image applications. But CIECAM02 has to use the reference white in model's prediction. That problem makes CIECAM02 hard to use with general digital images because there are not reference white data attached with digital images. This thesis thus tried to estimate the reference white from digital images by using reference white estimation models (Gray world and White patch), standard reference white (D65), and the white point of the viewing monitor, so as to find the parameter that can be used with unknown reference white images to make CIECAM02 predict the exact result.

CHAPTER III

EXPERIMENT

3.1 Apparatus

    3.1.1 CRT monitor

        Model: LaCIE Blue Electr22B4

        Size: 22 inches (view available: 20 inches)

        Maximum resolution: 2048 x 1536 dpi

        Dot pitch: 0.24 mm.

    3.1.2 Power PC Intel Pentium III processor

    3.1.3 Spectrophotometer: Gretag Macbeth spectrolino scan

    3.1.4 Calibration software: Profile Maker Pro 5.0

3.2 Experimental setup

3.2.1 Monitor calibration and characterization

The CRT monitor was calibrated using Profile Maker pro version 5.0 with its white point set to CIE illuminant D50. It was then characterized using the GOG model[29]. The performance of monitor characterization was tested based on 27 color patches that were generated from combinations of RGB (0, 127, 255) values. It was found to be $\Delta E^*_{ab} = 0.71 \pm 0.51$.

3.2.2 Original images

Three images were selected from a set of ISO standard images. The images are shown in Fig. 3.1. The first scene, "Fruits", is a high saturation picture containing many kinds of fruits in a brown basket. The second scene, "Wine", is an achromatic picture. The third scene, "Orchid", is a high contrast picture containing a white dish on a dark background.
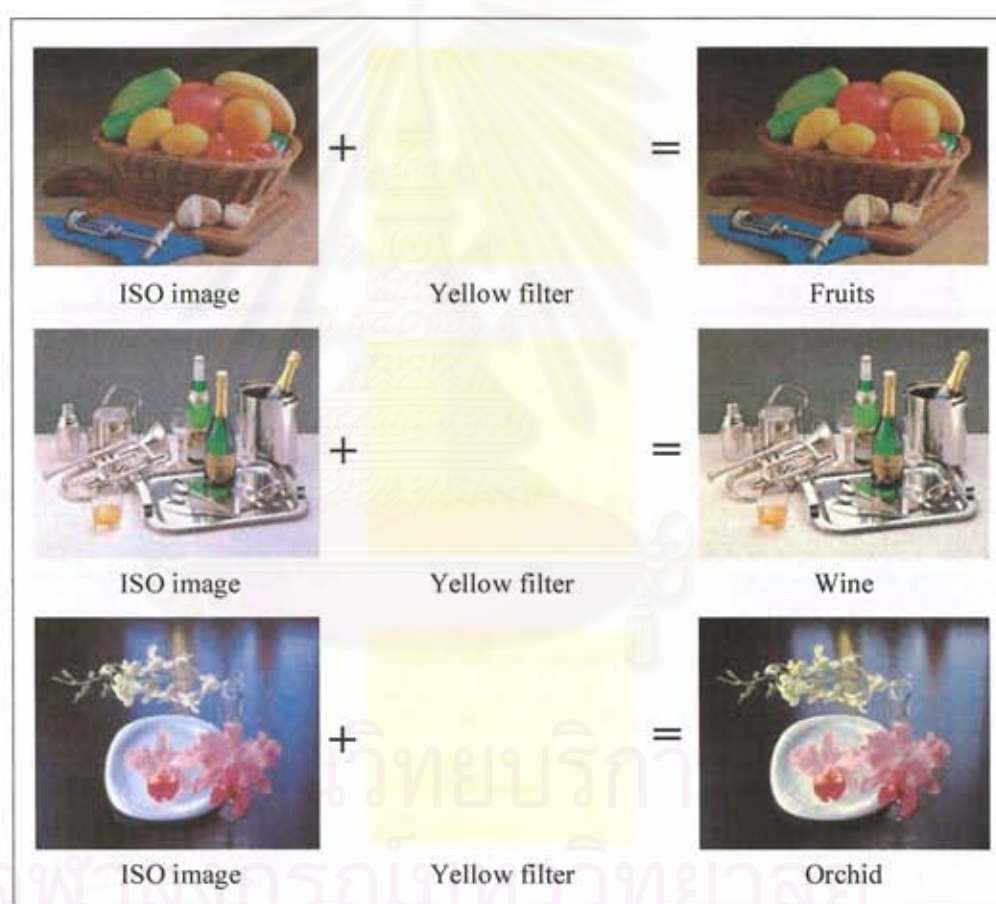
Fig. 3.1 Experimental original images obtained from applying yellow filters to the ISO images.

3.2.3 Reproduction images

The original images were processed through the CIECAM02 color appearance model to obtain reproduction images. In this experiment, four reference whites were input to the forward CIECAM02 model: white patch (WP), gray world (GW), CIE Illuminant D65 (D65) and white point of the CRT monitor (CRT). Thus, four reproduction images were produced for one original images' scene. The total number of reproduction images generated was then 12 (4 models x 3 scenes). The estimation methods to obtain the four difference reference whites used in the forward model of CIECAM02 are described below.

White patch (WP)

The maximum values of channels R, G and B (R_{max}, G_{max}, B_{max}) of the original image were used as a reference white. By using GOG model, the RGB data were transformed to XYZ tristimulus values ($X_w Y_w Z_w$).

$$R_{max}, G_{max}, B_{max} \xrightarrow{\text{GOG model}} X_w Y_w Z_w$$

Gray world (GW)

Based on the gray world theory[4], the average values of channels R, G and B of the original image were taken to be the reference white. The average RGB were processed via the GOG model to obtain the XYZ tristimulus values

(XYZ). After that, the XYZ tristimulus values were transformed to the CIE chromaticity coordinates (xy). The xy chromaticity coordinate of that color was then used as a chromaticity coordinate of the reference white. The XYZ tristimulus values of the reference white ($X_w Y_w Z_w$) were estimated from that chromaticity coordinate with a maximum luminance factor (Y_W) of 100.

$R_{average}$, $G_{average}$, $B_{average}$ $\xrightarrow{\text{GOG model}}$ XYZ $\longrightarrow$ xyY

$X_w Y_w Z_w$ $\longleftarrow$ $xyY_w (Y_w=100)$
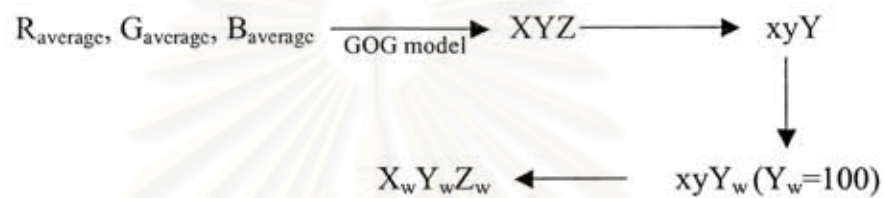
The chromaticity coordinates (xy) were calculated using Equation 3.1 and Equation 3.2.

$$x = X/(X+Y+Z) \qquad (3.1)$$

$$y = Y/(X+Y+Z) \qquad (3.2)$$

CIE Illuminant D65 (D65)

The XYZ tristimulus values of the CIE Illuminant D65 were used directly as the reference white.

$$X_w Y_w Z_w = 95.05, 100, 108.88$$

White point of the monitor (CRT)

The maximum RGB (255, 255, 255) values of the monitor were processed via the GOG model to obtain the XYZ tristimulus values. The XYZ values were then used as the reference white.

$$R_wG_wB_w \text{ (255, 255, 255)} \xrightarrow[\text{GOG model}]{} X_wY_wZ_w$$

For the WP and GW, the reference whites are image-dependent, while the reference white of the D65 and the white point of the testing monitor are constant values for all of the images. The reference whites were used as input parameters in CIECAM02 are summarized in Table 3.1.

Table 3.1 The reference whites used in forward CIECAM02.

| Model | Reference whites | | | | | | | | |
| | Fruits | | | Wine | | | Orchid | | |
	X	Y	Z	X	Y	Z	X	Y	Z
WP	43.20	45.93	26.09	92.87	98.10	63.97	91.30	97.33	55.73
GW	117.34	100	62.64	96.55	100	62.64	100.56	100	76.54
D65	95.05	100	108.88	95.05	100	108.88	95.05	100	108.88
CRT	96.69	100	84.03	96.69	100	84.03	96.69	100	84.03

The reference white is not the only parameter required in CIECAM02, but there are three parameters that needed to use together with the reference white: Luminance of adapting field (L_A), Luminance of background (Y_b), and Surrounding. The estimation of each parameter is described below and the input data of each parameter are shown in Table 3.2.

Luminance of adapting field (L_A)

The luminance of adapting field or L_A was calculated from the average luminance of the scene by using Equation 3.3 where Y is the average Y tristimulus values of original images; L is the absolute luminance of white point of the monitor. For this experiment, the monitor had luminance of 102.7 cd/ m^2.

$$L_A = \frac{YL}{100} \qquad (3.3)$$

Background luminance (Y_b)

For the experiment, the images were displayed full frame on the monitor. There was no real background; hence, the background luminance (Y_b) was set, in all cases, to at 20, that is the general value of background luminance, implicitly assuming a gray world assumption.

Surrounding

Surrounding was set up to dim surround, which includes three parameters; factor for degree of adaptation (F) was set to 0.9, chromatic induction factor (N_C) was set to 0.9, and impact of surround (c) was set to 0.59 in all cases.

Table 3.2 The input viewing condition parameters of each image in each model.

Images	Input viewing condition parameters		
	L_A	Y_b	Surround
Fruits	9.42	20	Dim
Wine	33.49	20	Dim
Orchids	15.42	20	Dim

3.2.4 Generation of reproduction images

Fig. 3.2 shows a flow chart of processing reproduction images. The explanation for each step of image processing is as follows.

Step 1: The RGB data of the original images were converted to XYZ data based on a pixel-by-pixel basis using the forward GOG model.

Step 2: The XYZ data were processed via the forward CIECAM02 model using four different reference whites. The JCh data were then obtained.

Step 3: The JCh data were transformed back to the XYZ tristimulus values (X'Y'Z') via the inverse CIECAM02 model with S_E as the reference white ($X_w=Y_w=Z_w=100$).

Step 4: The X'Y'Z' data were then converted to RGB data using the inverse GOG model. The original images together with the reproduction images used in the experiment are shown in Fig. 3.3.
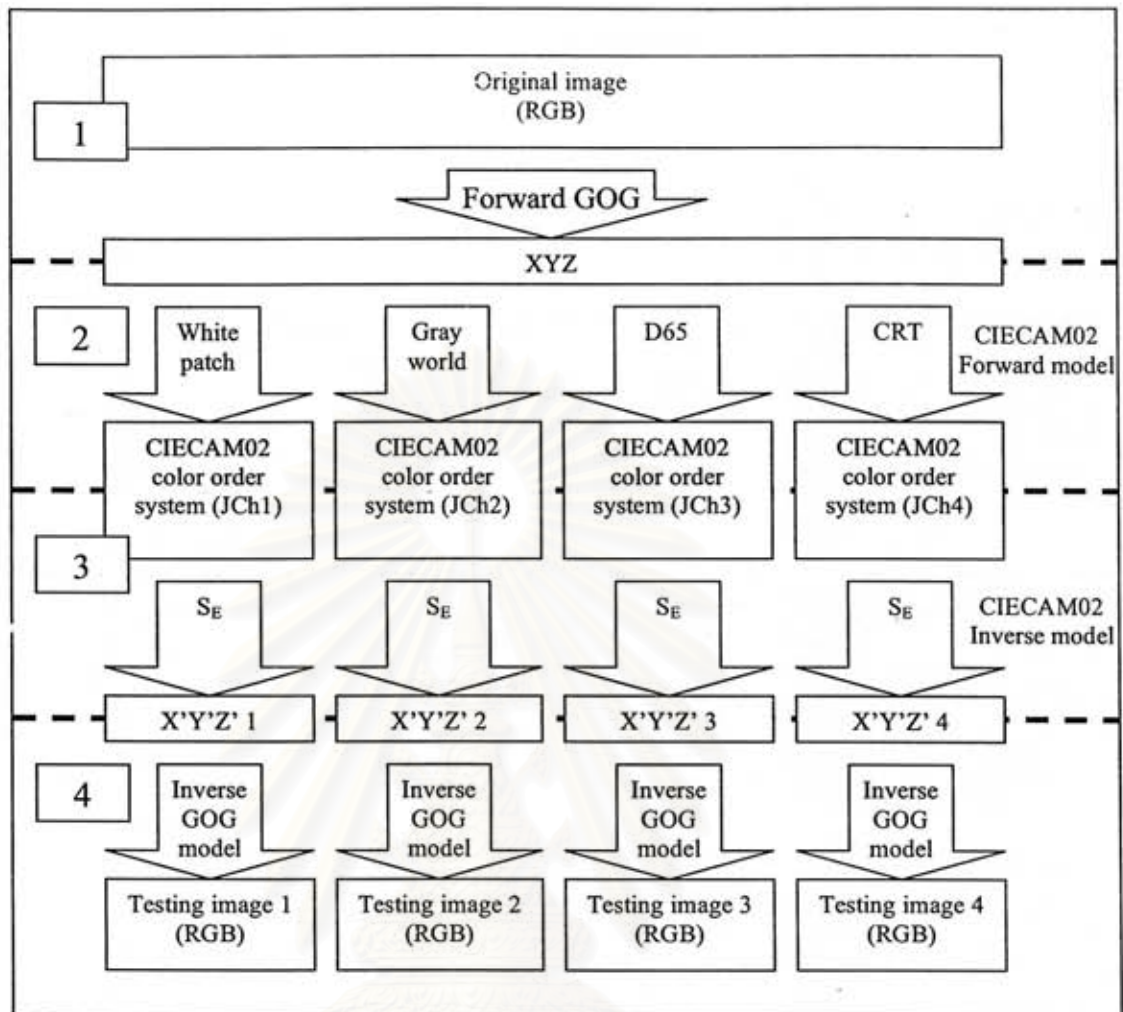
Fig. 3.2 A flow chart of image processing.

Fig. 3.3 The original images and the reproduction images used in the

experiment.

3.2.5 Viewing configuration

The original images and the reproductions were displayed on a calibrated CRT monitor LaCIE Blue Electr22B4 at 72 dpi. All images had the same physical size of 12 inches x 16 inches, which covered the whole screen of the monitor. The white point of the CRT was set to the CIE Illuminant D50.

An observer sat approximately 35 inches away from the CRT screen in a darkened room, as shown in Fig. 3.4.
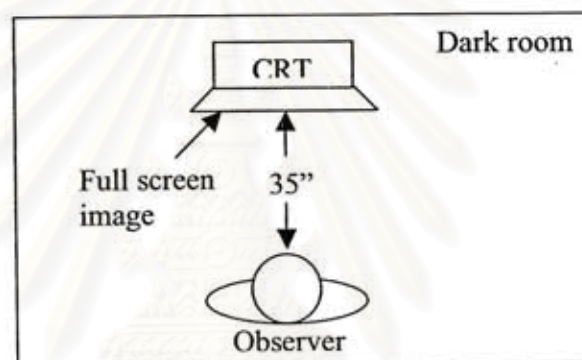
Fig. 3.4 Viewing configuration.

3.3 Psychophysical experiments

Fifteen observers, 9 males and 6 females, between ages of 20 to 24, undertook the color blindness test to ensure that they had normal color vision before carrying out the experiments. Observers had to compare the original image to a set of reproduction images using the memory viewing technique[34]. Observers made a judgment in terms of how well the colors in the images matched the originals using a 1-7 integer scale, where 1 was defined as a complete mismatch, 2, very serious mismatch, 3, serious mismatch, 4, an acceptable match, 5 close match, 6 very close match and 7, a perfect match.

The numbers in between represented the equal differences of a color match between the neighboring categories. The original images were displayed on the monitor for 2 minutes, followed by four reproduction images, each for 1 minute. Before changing to the next image, a uniform black image was displayed to eliminate the effect of afterimage and to aid the full adaptation of the next image. The reproduction images were displayed in a random order. All images were displayed using Irfanview software[40]. An observer spent approximately 30 minutes to perform three sets of experimental images. First, the observer practiced on how to make judgments for about 3 minutes. Three sets of experimental images were then presented in a random order to the observer. Each observer spent around 9 minutes to complete one set of experimental images.

CHAPTER IV

RESULTS AND DISCUSSIONS

4.1 Experimental data

Three digital images with unknown reference whites were used as original images in this study. Four models: White patch (WP), Gray world (GW), CIE Illuminant D65 (D65) and white point of the monitor (CRT), were used to estimate the reference whites of the original images. The reproduction images were produced via CIECAM02 with the reference white obtained from each model. The images reproduced from closely estimated reference whites would match the originals. The degree of color matches indicates the performance of the model.

Fifteen observers made a judgment in terms of how well the colors in the reproduction images matched the originals using a 1-7 integer scale, where 1 was defined as a complete mismatch, 4, an acceptable match, and 7, a perfect match. Two approaches were used for data analysis. First, an average of observer raw data was used directly. The other way was to use the Law of Category Judgment[35] to transform the raw data onto an interval scale. The results are called z-scores indicating model's accuracy.

The accuracy of z-score values was described in terms of a 95% confidence interval, which can be calculated by

$$\mu \pm \frac{1.96\sigma}{\sqrt{N}} \qquad (4.1)$$

where μ is the mean value of z-scores. N is the number of observations from an image sample. Because one unit on the interval scale equals $\sqrt{2}\sigma$, the standard deviation, σ, of a given value is $\frac{1}{\sqrt{2}}$ units. Therefore, the 95% confidence scale can be calculated by $\mu \pm \frac{1.39}{\sqrt{N}}$. For instance, to calculate the averaged results in All images (results combined from three images), N = 45 (15 observers x 3 images). Thus, the confidence interval around each z-score value was 0.21. If the mean of one model overlaps another model's confidence interval, the two models are considered not to be significantly different and can lead to the same conclusion.

The experimental raw data are presented in terms of the frequencies of times an image was placed in each category and are shown in Table 4.1.

Table 4.1 Experimental raw data.

Images	Model	Scores						
		1	2	3	4	5	6	7
Fruits	WP	0	0	2	6	3	4	0
	GW	0	1	7	6	1	0	0
	D65	0	0	0	1	2	6	6
	CRT	0	0	0	1	5	7	2
Wine	WP	0	1	1	1	8	3	1
	GW	0	0	2	3	4	5	1
	D65	0	0	2	1	2	6	4
	CRT	0	0	1	2	4	7	1
Orchid	WP	0	1	1	4	5	4	0
	GW	0	0	2	2	4	6	1
	D65	0	0	1	3	6	4	1
	CRT	0	0	0	3	2	5	5

4.2 Observer accuracy

The observer accuracy was estimated using a coefficient of variation (CV) measure. This measure indicates an agreement between two sets of data, which can be computed as shown in Equation 4.2. In this study, an agreement between each observer's result and the mean result calculated from all observers represents the observer accuracy. Thus, the variables in Equation 4.2 are described as follows: n is the number of observations, x_i is the individual's result, and $\bar{x}$ is the mean value of all observers' scores. A CV value of 20 means 20% error of individual from the mean. The results for observer accuracy are summarized in Table 4.2.

$$CV = \frac{100\sqrt{\dfrac{\sum (x_i - \bar{x})^2}{n-1}}}{\bar{x}} \qquad (4.2)$$

Table 4.2 Coefficient of Variation (CV %) of observers

	WP	GW	D65	CRT	Mean
Fruits	23	21	15	14	**18**
Wine	25	24	24	20	**23**
Orchids	25	23	20	20	**22**
Mean	**24**	**23**	**20**	**18**	**21**

Considering an impact of image content on observer accuracy from Table 4.2, it can be seen that "Wine" has the highest mean CV of 23, followed by "Orchids" (22) and "Fruits" (18). The difference between mean CV values across images was 5%, revealing that the models' performance was affected by image content. "Wine" containing mainly neutral colors was found to be most difficult to judge, implying that all modes' performed similarly. On the other hand, the image with color variety "Fruits" had low observer error because the reproduction images were distinctly different and thus easy to categorize. For the observer accuracy for each model, the maximum CV was found for WP (24), followed by GW (23), D65 (20), and CRT (18). This result shows that WP and GW were most image-dependent, while D65 and CRT showed consistent performance across images. The overall mean of observer errors was 21%, which considered quite reasonable. This is mainly due to the nature of visual experiments using category judgment and memory matching techniques. An ability to memorize color for each observer was different. The criteria for which each observer used were also different. Some of observers gave priority to hue while judging the images. Some may have used brightness.

4.3 Model's performance

The results indicating the model's performance, which include an average of categories (Mean), z-scores on an interval scale, and rank order of model's performance, are summarized in Table 4.3. For each model, a rank was given by comparing z-score results among different models using 95% confidence interval criteria. Discussions of the results for each image and the results combined from all images are given in the following sections.

Table 4.3 A summary of model's performance.

Images		Model				95%CL
		WP	GW	D65	CRT	
Fruits	Mean	4.60	3.47	6.13	5.69	
	z-scores	1.97	1.15	2.98	2.74	0.36
	Rank	2	3	1	1	
Wine	Mean	4.93	5.00	5.60	5.33	
	z-scores	2.00	2.11	2.43	2.30	0.36
	Rank	1	1	1	1	
Orchids	Mean	4.67	5.13	5.07	5.80	
	z-scores	1.79	2.19	2.19	2.67	0.36
	Rank	3	2	2	1	

4.3.1 Fruits

From Table 4.3, D65 has the highest mean value followed by CRT, WP and GW, respectively. The mean values indicate that D65 and CRT provided good color matches while WP and GW gave an acceptable match and a poor match, respectively. This result agreed with the result from z-scores, where an descending order of z-scores was exactly the same as that of the mean values,

i.e. D65, CRT, WP, and GW. However, when considering the 95% confidence interval, it was found that D65 and CRT were in the same rank (Fig. 4.1), indicating that the two models gave similar degrees of color matches.

Fig. 4.1 Models' performance of each model in "Fruits"
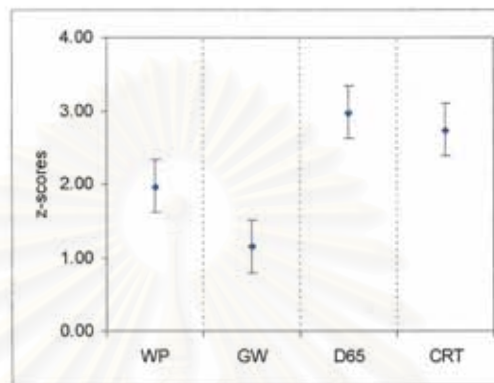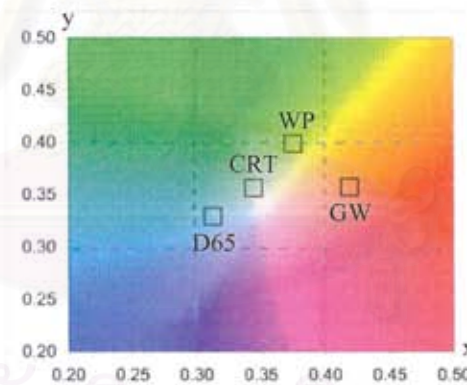

Fig. 4.2 Chromaticity coordinates (xy) of each reference white for "Fruits"

Fig. 4.2 shows colors of reference whites estimated by each model tested. The CIECAM02 model required a reference white as one of input parameters in order to compensate changes of color appearance due to the color of light source under which the sample is viewed. This is because the chromatic

adaptation mechanism in the human visual system attempting to retain color appearance of the sample as when viewed under daylight. Thus, when chromatic adaptation takes place, as assumed in CIECAM02, the color of light source is removed from the sample.

As can be seen from Fig. 4.2, a reference white estimated by GW was more reddish than those of other models. This resulted in the reproduction image predicted by CIECAM02 becoming too bluish. On the other hand, the reference whites of D65 and CRT were very close and not much different from the equal energy white (S_E); therefore, the reproduction images were still yellowish. The reason why these two models gave the best performance could be that the state of chromatic adaptation was incomplete, so the color of light source could not be completely removed. The yellowish images would therefore provide closer matches to the original yellowish images.

4.3.2 Wine

From Table 4.3, D65 has the highest mean value (5.60) followed by CRT (5.33), GW (5.00) and WP (4.93). However, the results of z-scores showed that all models had very similar performance, as the mean z-scores of each model overlapped other models' confidence intervals (Fig. 4.3). This leads to the result that all models provided reasonable matches to the originals: no model perform better than any others.

Reference whites estimated by each model are showed in Fig. 4.4. It can be seen that reference whites of WP and GW are very similar and slightly yellowish. Since most colors in "Wine" are neutral, the deviation from a neutral color of reference whites is the impact of light source's color. Note that reference whites of D65 and CRT are image-independent, i.e. they are constant for all images tested, while the reference whites of WP and GW are image-dependent. This implies that GW and WP work well for neutral images or images that amounts of each color contained in the images are about the same.
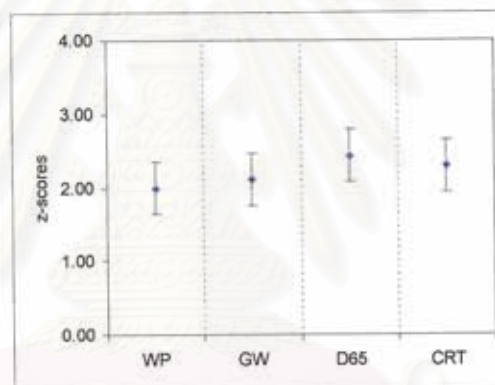
Fig. 4.3 Models' performance of each model in "Wine"
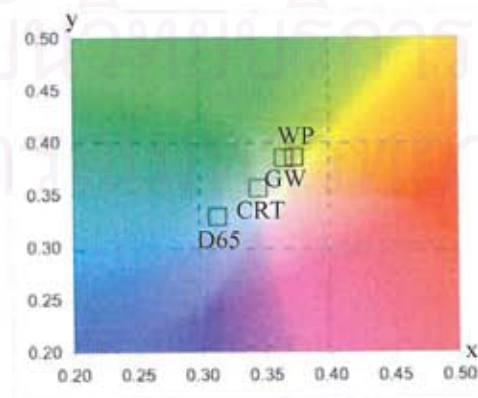
Fig. 4.4 Chromaticity coordinates (xy) of each reference white for "Wine"

4.3.3 Orchids

The results from Table 4.3 showed that CRT provided the best match, followed by GW, D65, and WP, respectively. GW performed as well as D65 for "Orchids" (Fig 4.5). However, the reference white of GW was closer to CRT than that of D65 (Fig. 4.6).
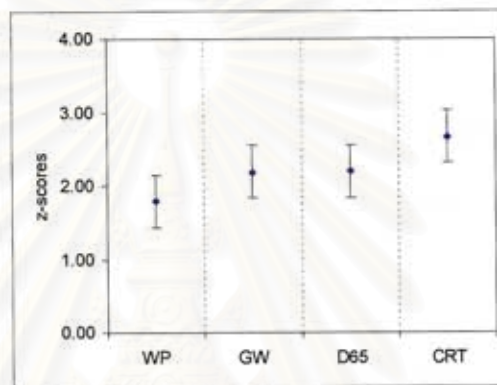
Fig. 4.5 Models' performance of each model in "Orchids"
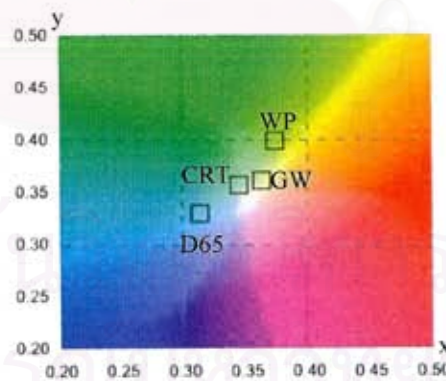
Fig. 4.6 Chromaticity coordinates (xy) of each reference white for "Orchids"

"Orchids" is a high contrast image containing a white dish on a black background. The white dish was the key that observers used to consider the

reproduction images. Therefore, the dish should not be too yellowish or too bluish. Fig. 4.6 shows that the reference white of D65 is slightly bluish while that of CRT is slightly yellowish. When the bluish reference white of D65 was input into CIECAM02, the model interpreted the yellow color casting over the entire image as the actual color of the objects in the image. CIECAM02 thus predicted the reproduction image with the dish in particular to be too yellowish. On the contrary, when the input reference white was too yellowish, CIECAM02 interpreted that the yellow color came from the light source and removed it from the image. Thus the dish of the reproduction image obtained from WP became too bluish.

4.3.4 All images

For this section, mean values and z-scores of all images were averaged to consider overall performance regarding how well each model estimated the reference white to be applied to CIECAM02, as to producing close color matches to originals. The results are summarized in Table 4.4. The models' performance for each model (z-scores) is plotted in Fig. 4.7.

Table 4.4 The averaged mean value, z-scores and a rank of each model

		WP	GW	D65	CRT	95%CL
All images	Mean	4.73	4.53	5.60	5.60	
	z-scores	1.92	1.82	2.54	2.57	0.21
	Rank	2	2	1	1	
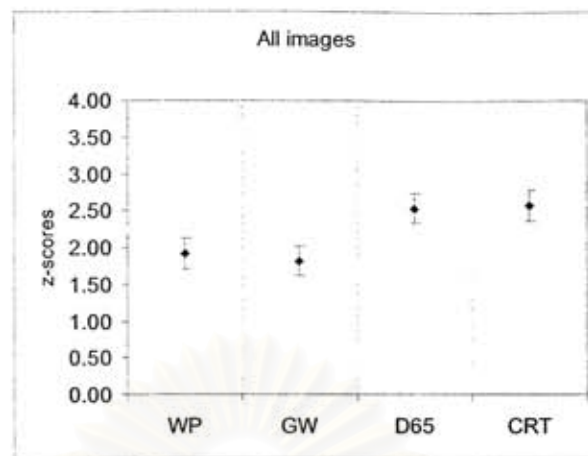
Fig. 4.7 Models' performance in all images (averaged from all of experimental images).

The results from all images combined showed that WP and GW reference whites gave similar results. Both models provided "close match" to the original. D65 and CRT also gave similar results and outperformed WP and GW. This might be due to the fact that the state of chromatic adaptation was incomplete; therefore, the human visual system could not completely remove the yellow cast. The images were still perceived as yellowish. The WP and GW models might estimate so yellowish reference whites that CIECAM02 removed too much yellow from the images, resulting in too less yellowish, or too bluish in some cases, or too bright images. In the case of D65 and CRT, both models gave near equal energy white (S_E). Hence, the reproduction images were still yellowish as little was removed as a result of CIECAM02, which yielded closer matches to the originals.

4.4 Image dependency

The performance of each model for each image is compared in Fig. 4.8 so as to evaluate the degree of image dependency for each model.
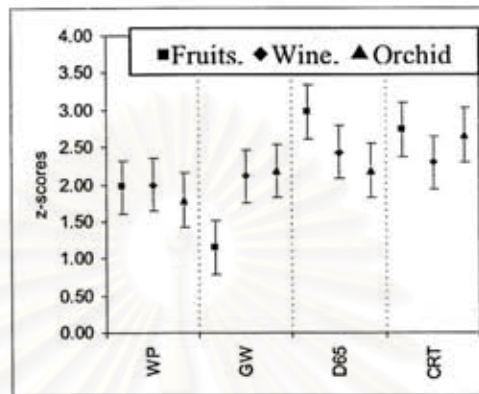
Fig. 4.8 Models' performance for each image

The performance of some models might highly depend on images, e.g. a model could give very close color match for some types of images but very poor match for other types. Such a model would not be desirable in general and careful consideration should be taken when using such the model. From Fig. 4.8, it can be seen that the performance of GW spreads out quite widely in comparison with other model's. In this study, a quantitative measure of the degree of image dependency was obtained by calculating differences between the highest and lowest z-scores for each model. The results are shown in Table 4.5.

Table 4.5 The degree of image dependency (Δz) for each model

	WP	GW	D65	CRT
Image dependency	0.21	1.04	0.78	0.44

From Table 4.5, WP has the lowest image dependency, indicating that WP will give similar performance for all types of images. GW is considered to be inconsistent, as can be seen in Fig. 4.8 that it performed badly for "Fruits".

4.5 Comparisons between z-scores and image dependency

In general, the good performing model should provide good color matches for all types of images. That means the model should have high model's accuracy (z-scores) and low image dependency (Δz). If a model has low image dependency but poor model's accuracy, it should not be used for any images. However, a model that has high image dependency and also high or reasonable model's accuracy, it can be used for some types of images. Hence, both model's accuracy and image dependency need to be considered in order to correctly select the model to be used.
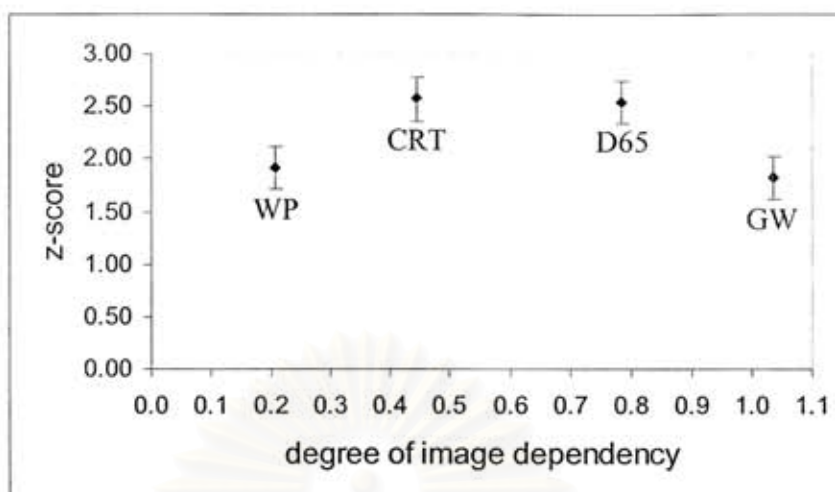
Fig. 4.9 The correlation between model's accuracy (z-scores) and image dependency (Δz)

Fig. 4.9 shows a plot between model's accuracy and image dependency. The results showed that although WP and GW gave similar performance, WP had the best image dependency while GW had the worst. This indicates that GW can be used for some types of images while WP is not recommended for any. D65 had high model's accuracy as well as image dependency. On the other hand, CRT showed good performance with reasonably low image dependency.

Note that the original images as well as the reproduction images covered the full frame of the monitor. The adapting fields varied for each image, depending on color contents in an image. As a result, the degree of chromatic adaptation was different for different images. This could explain why a fixed reference white such as D65 gave inconstant performance over the images tested. For example, the chromatic adaptation was more complete for

"Orchids" than that for "Fruits" because there were more neutral colors in "Orchids". The human visual system was able to discount more amount of yellow cast on "Orchids" than "Fruits". Thus the use of D65 as a reference white yielded too yellowish reproduction image for "Orchids" while giving a close match for "Fruits", as CIECAM02 removed the same amount of yellowness from both images.

All in all, a proper reference white to be applied to CIECAM02 should be image-dependent. This is because even the best performing model, i.e. CRT, did not produce "a very close match" for all types of images tested. The reason why CRT performed best for all images could be that the originals were all perturbed with yellow color and the chromatic adaptation was not complete when viewed these images, which resulted in the perception of yellowish originals. The white point of the CRT was set to D50, which is slightly yellowish. Therefore, when input D50 as the reference white to CIECAM02, little amount of yellowness was removed and yellowish reproduction images were obtained, which provided good color matches to the originals. If the originals were perturbed with other colors, the results might be different.

CHAPTER V

CONCLUSIONS AND SUGGESTIONS

5.1 Conclusions

To obtain color matches of images viewed under difference viewing conditions, the use of color appearance models is needed in a process of color image reproduction. However, to successfully implement a color appearance model, a certain number of input parameters is required, and one of the important parameters is a reference white. For images captured with digital cameras, reference whites are often unknown. Hence, the aim of this thesis was to investigate the means of applying color appearance models to images with unknown reference whites. The CIECAM02 color appearance model was selected because it has been recommended by the CIE. The investigation was done by estimating reference whites of digital images using two methods, i.e. gray world (GW) and white patch (WP), a standard reference white, i.e. D65, and the white point set to display the images on a CRT monitor, i.e. D50. Thus, four different reference whites estimated by four different models, i.e. white patch (WP), gray world (GW), the CIE illuminant D65 (D65) and the white point of testing monitor (CRT), were tested to be used as the parameter in CIECAM02. Images reproduced via CIECAM02 with suitable reference whites would give good color matches to the original images. The degree of color matches indicated the accuracy of reference-white estimation models tested in

conjunction with CIECAM02 in color image reproduction. Three different images were tested in the study, so as to investigate the impact of image contents on the performance of the estimation models. Fifteen observers participated in visual experiments in involving the memory matching and the category judgment techniques. The major findings of this study are as follows:

- The performance of the reference-whites estimation methods depended on the types of images used. Even for the methods that their reference white were changeable according to image content, their performance were inconsistent.

- White patch that got the reference white from the maximum values of channels R, G and B of the images was the method that had the lowest degree of image dependency but the overall results of White patch was " Close match" which was not the best performance among models tested.

- Gray world was the method that assumed the reference white from the average value of channels R, G and B. It had the highest degree of image dependency, means that the performance of this method depends on the image content.

- Gray world performed well for "Wine", the image with mainly neutral colors. However, it did not work well for the colorful image "Fruits".

- The CIE illuminant D65 was image-dependent. High degree of image dependency was found for this method. The performance of D65 was

very good for the colorful image (Fruits) but for the other cases its performance was not better than the other models.

- The white point of the monitor (CRT) was the method that had low degree of image dependency. It was found that this method gave "Very close match" for "Fruits" and "Orchids", and "Close match" for "Wine".

In conclusion, the white point set for the CRT monitor used to display images is recommended for applications of CIECAM02 for general images that their reference whites were unknown. This recommendation is based on the results showing that the CRT method provided good color match with reasonably low image dependency.

5.2 Suggestions

A reference white of an image displayed and covered the full screen of a monitor is expected to depend on color contents of the image due to the fact that the chromatic adaptation is dependent on the scene content. However, the results from this thesis showed that the reference white estimation models that are image-dependent did not give the good performance for all images. This might be because the chromatic adaptation was not complete when viewed the originals. In the case of the good performing model CRT, the white point of the monitor was set to CIE illuminant D50 that is slightly yellowish, little yellowness was removed and yellowish reproduction images were obtained, which provided good color matches to the originals. Note that yellowish

images were used as the originals in this thesis; thus different results might be obtained if the experimental images were changed. Further work should consider other methods of estimating reference whites and more kinds of images as well as changing the filter that was used to produce original images to other colors such as green or red filter.

REFERENCES

1. Luo, M. R., Hunt, R. W. G. The Structure of the CIE 1997 Colour Appearance Model (CIECAM97s). <u>Color Res. Appl.</u> 23 (1997): 138-146.

2. Moroney, N., Fairchild, M. D., Hunt, R. W. G., Li, C. The CIECAM02 colour appearance model, <u>Proceeding of The 10th Color Imaging Conference: CIC 2002</u> (2002): 23-27.

3. Li, C., Luo, M. R., Hunt, R. W. G., Newman, T. The performance of CIECAM02, <u>Proceeding of The 10th Color Imaging Conference: CIC 2002</u> (2002): 28-32.

4. Buchsbaum, G. A Spatial Processor Model for Object Colour Perception, <u>J. Franklin Institute</u> (1980): 1-26.

5. Cardei, V. C., Funt, B., and Barnard, K. White point estimation for uncalibrated images, <u>Proceeding of The 7th Color Imaging Conference</u> (1999): 97-100.

6. Land, E. H. The Retinex Theory of Color Vision, <u>Scientific American</u> (1977): 108-129.

7. Funt, B., Bernard, K., and Martin, L. Is machine color constancy good enough? <u>Proceedings of The 5th European Conference on Computer Vision (ECCV' 98)</u> (1998): 445-459.

8. Vlad C. Cardei, Brian V. Funt, Kobus Barnard. White point estimation for uncalibrated images. <u>Proceeding of The 7th Color Imaging Conference: CIC 1999</u> (1999): 97-100.

9. Danger, E. P. The Color Handbook. Aldersot: Gower Technical (1987): 4.

10. Berns, R. S. Principles of Color Technology. 3rd Ed. New York: John Wiley & Sons (2000): 13-17.

11. Billmeyer, Jr., F.W. and Saltzman, M. Principle of Color Technology, 2nd Ed. New York: John Wiley & Sons, (1981): 17.

12. Bern, R.S. Principle of Color Technology, 3rd Ed. New York John: Wiley & Sons. (2000): 56-69.

13. Chrisment A. Color & Colorimetry, Editions 3C Conseil, Paris (1998): 115.

14. Fairchild, M. D. Color Appearance Models, 2nd Ed. USA: Addison Wesley Longman (1997): 132-178.

15. Fairchild, M. D. Color Appearance Models: CIECAM02 and Beyond [Online]. Available from: http://www.cis.rit.edu/fairchirld/PDFs/AppearanceLec.pdf [2004, March 17].

16. Albers, J. Interaction of color, Yale University Press, New Haven, Conn. (1963).

17. Hurvich, L. M., Jameson, D. A psychophysical study of white. III. Adaptation as a variant, J. Opt. Soc. Am. 41 (1951): 787-801.

18. Boynton, R. M. Human Color Vision, Optical Society of America, Washington D.C. (1979).

19. R. M. Evans, An Introduction to Color, New York, N.Y. John Wiley & Sons, (1948).

20. Cornelissen, F. W. Brenner, E. On the role and nature of adaptation inchromatic induction, <u>Channels in the Visual Nervous System: Neurophysiology, Psychophysics and Models</u>, Freund Publishing, London (1991): 109-123.

21. Blackwell, K. T., Buchsbaum, G. <u>The effect of spatial and chromatic parameters on chromatic induction</u>, Color Res. Appl. 13 (1988): 166-173.

22. Robertson, A. R. Figure 6-2 presented at the 1996 ISCC Annual Meeting, Orlando, Fla. (1996).

23. Hunt, R. W. G. Light and dark adaptation and the perception of color, <u>J. Opt. Soc. Am.</u> 42 (1952): 190-199.

24. Stevens, J. C., Stevens, S. S. Brightness functions: Effects of adaptation, <u>J. Opt. Soc. Am.</u> 53 (1963): 375-385.

25. Abramov, I., Gordon, J., Chan, H. Color appearance across the retina: Effects of a white surround, <u>J. Opt. Soc. Am.</u> A 9 (1992): 195-202.

26. Hunt, R. W. G. Revised color-appearance model for related and unrelated color, <u>Color Res. Appl.</u> 16 (1991): 146-165.

27. Hunt, R. W. G. <u>The Reproduction of Color</u>, 5th Ed. England: Fountain Press, (1995).

28. CIE, Colorimetry <u>CIE Publ.</u> No. 15.2, Vienna (1986).

29. Hunt, R. W. G. <u>Measuring colour</u>, 2nd ed., New York: Ellis Horwood (1991).

30. Biggs, B. Figure presented at [Online] http://scanline.ca/ciecam02, [2004, March 17].

31. Luo, M. R., et al. Quantifying colour appearance. Part I. LUTCHI colour appearance data, Color Res. Appl. 16 (1991): 166-180.

32. Hunt, R. W. G., Pointer, M. R. A colour-appearance transform for the 1931 standard colorimetric observer, Col. Res. Appl. 10 (1985): 165-179.

33. Mechaelis, L., Menten, M. L. Die Kinetik der Invertinwerkung, Biochemische Zeitschrift, 49 (1983).

34. Valeton, J. M., Norren, D. van, Light adaptation of primate cones: an analysis based on extracellular data, Vision Res. 23, 12, (1983): 1539-1547.

35. Karen M. Braun, Mark D. Fairchild, Paula J. Alessi. Viewing Techniques for Cross-Media Image Comparisons. Color Res. Appl. 23 (1996): 6-17.

36. Bartleson, CJ., Grum, F. Optical radiation measurements, New York: Academic Press (1984): 441-456.

37. Torgerson, WS, Theory and methods of scaling. New York: Wiley (1958).

38. Thurstone, L. L. A law of categorical judgment, Phychol. Rev. 34 (1927): 237-286.

39. Mosteller, F. Remarks on the method of paired comparisons: 1. The least squares solution, assuming equal standard deviations and equal correlations. Phychometrika 16 (1951): 3-9.

40. http://www.irfanview.com [Online], [2004, March 17].

APPENDIX A

Steps for calculation of CIECAM02 inverse model

CIECAM02 Inverse Model

Input Data;

1. Color appearance data (J, C, h)

2. Reference white (X_w, Y_w, Z_w)

3. Luminance of adapting field $(L_A, cd/m^2)$

4. Relative luminance of Background (Y_b)

5. Surround (F, c, N_c)

Step-1 Calculate A, e and t

$$A = A_W \left((J/100)^{(1/cz)} \right)$$

$$e = \left(\left(\frac{12500}{13} \right) N_c N_{cb} \right) \left(\cos \left(h \left(\frac{\pi}{180} \right) + 2 \right) + 3.8 \right)$$

$$t = \left(\frac{C}{\sqrt{\frac{J}{100}} \left(1.64 - 0.29^n \right)^{0.73}} \right)^{\left(\frac{1}{0.9} \right)}$$

where A_w can calculated by CIECAM02 Forward model

Step-2 Calculate a, b

If t = 0;

a = 0, b = 0

If $\left| \sin \left(\frac{h\pi}{180} \right) \right| \geq \left| \cos \left(\frac{h\pi}{180} \right) \right|$

$$a = \left| \frac{\left(\dfrac{A}{N_{bb}} + 0.305\right)\left(2 + \dfrac{21}{22}\right)\left(\dfrac{460}{1403}\right)}{\left(\dfrac{\left(\dfrac{e}{t}\right)}{\sin\left(\dfrac{h\pi}{180}\right)} + \left(2 + \dfrac{21}{20}\right)\left(\dfrac{220}{1403}\right)\left(\dfrac{\cos\left(\dfrac{h\pi}{180}\right)}{\sin\left(\dfrac{h\pi}{180}\right)}\right) - \left(\dfrac{27}{1403}\right) + \left(\dfrac{21}{20}\right)\left(\dfrac{6300}{1403}\right)\right)} \right| \left(\frac{\cos\left(\dfrac{h\pi}{180}\right)}{\sin\left(\dfrac{h\pi}{180}\right)}\right)$$

$$b = \left| \frac{\left(\dfrac{A}{N_{bb}} + 0.305\right)\left(2 + \dfrac{21}{22}\right)\left(\dfrac{460}{1403}\right)}{\left(\dfrac{\left(\dfrac{e}{t}\right)}{\sin\left(\dfrac{h\pi}{180}\right)} + \left(2 + \dfrac{21}{20}\right)\left(\dfrac{220}{1403}\right)\left(\dfrac{\cos\left(\dfrac{h\pi}{180}\right)}{\sin\left(\dfrac{h\pi}{180}\right)}\right) - \left(\dfrac{27}{1403}\right) + \left(\dfrac{21}{20}\right)\left(\dfrac{6300}{1403}\right)\right)} \right|$$

If $\left|\sin\left(\dfrac{h\pi}{180}\right)\right| < \left|\cos\left(\dfrac{h\pi}{180}\right)\right|$

$$a = \left| \frac{\left(\dfrac{A}{N_{bb}} + 0.305\right)\left(2 + \dfrac{21}{22}\right)\left(\dfrac{460}{1403}\right)}{\left(\dfrac{\left(\dfrac{e}{t}\right)}{\cos\left(\dfrac{h\pi}{180}\right)} + \left(2 + \dfrac{21}{20}\right)\left(\dfrac{220}{1403}\right) - \left(\dfrac{27}{1403} - \left(\dfrac{21}{20}\right)\left(\dfrac{6300}{1403}\right)\dfrac{\sin\left(\dfrac{h\pi}{180}\right)}{\cos\left(\dfrac{h\pi}{180}\right)}\right)\right)} \right|$$

$$b = \left| \frac{\left(\dfrac{A}{N_{bb}} + 0.305\right)\left(2 + \dfrac{21}{22}\right)\left(\dfrac{460}{1403}\right)}{\left(\dfrac{\left(\dfrac{e}{t}\right)}{\cos\left(\dfrac{h\pi}{180}\right)} + \left(2 + \dfrac{21}{20}\right)\left(\dfrac{220}{1403}\right) - \left(\dfrac{27}{1403} - \left(\dfrac{21}{20}\right)\left(\dfrac{6300}{1403}\right)\dfrac{\sin\left(\dfrac{h\pi}{180}\right)}{\cos\left(\dfrac{h\pi}{180}\right)}\right)\right)} \right| \left(\frac{\sin\left(\dfrac{h\pi}{180}\right)}{\cos\left(\dfrac{h\pi}{180}\right)}\right)$$

Step-3 Calculate R_a, G_a, and B_a

$$R_a = \frac{460}{1403}\left(\frac{A}{N_{bb}} + 0.305\right) + \frac{451}{1403}a + \frac{288}{1403}b$$

$$G_a = \frac{460}{1403}\left(\frac{A}{N_{bb}} + 0.305\right) - \frac{891}{1403}a - \frac{261}{1403}b$$

$$B_a = \frac{460}{1403}\left(\frac{A}{N_{bb}} + 0.305\right) - \frac{220}{1403}a - \frac{6300}{1403}b$$

Step-4 Calculate R', G', and B'

$$R' = \left(27.13\left(\frac{R_a - 0.1}{400.1 - Ra}\right)\right)^{\left(\frac{1}{0.42}\right)}\left(\frac{100}{F_L}\right)$$

Step-5 Calculate R_C, G_C, and B_C

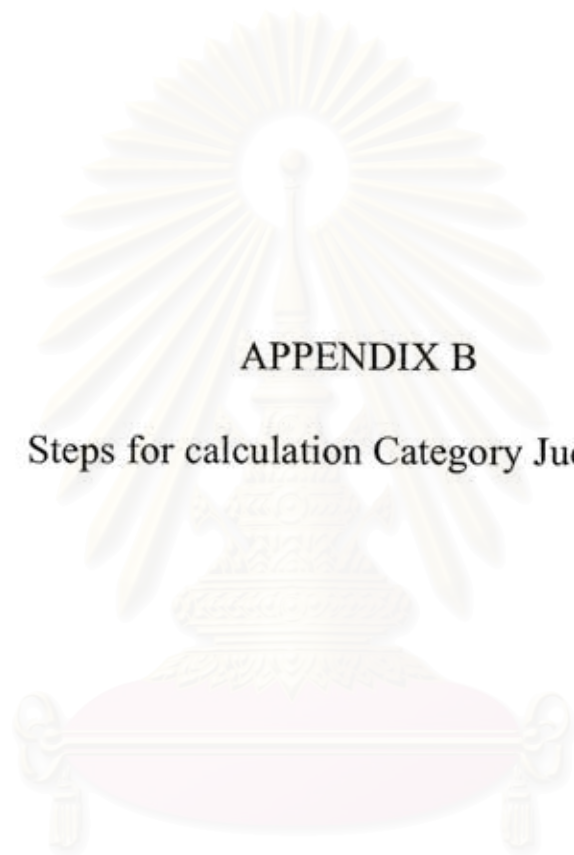$$\begin{bmatrix} Rc \\ Gc \\ Bc \end{bmatrix} = M_{CAT02}M_H^{-1}\begin{bmatrix} R' \\ G' \\ B' \end{bmatrix}$$

Step-6 Calculate R, G, and B

$$R = \frac{Rc}{D\dfrac{Y_W}{R_W} + (1-D)}$$

Step-7 Calculate XYZ tristimulus values

$$\begin{bmatrix} X \\ Y \\ Z \end{bmatrix} = M_{CAT02}^{-1}\begin{bmatrix} R \\ G \\ B \end{bmatrix}$$

APPENDIX B

Steps for calculation Category Judgment

Law of category judgment

The following is an example of data analysis of an experiment conducted using the categorical-judgment technique. The condition given here is that four observers categorized 3 images (A, B and C) into 1-7 integer scale in accordance with how well they matched to the original. Category 1 represents the worst match and 7 the best. Numbers in between represent equal interval of color matches. Note that the data used here are arbitrary and for the purpose of demonstrating the data analysis procedure described in Chapter 4.

First, the transformation between logistic functions and z scores was defined by plotting LG data against z scores and calculating an equation to fit the data, as shown in Fig. B.1. For the present example, 41 proportions between 0 and 1 (0.005, 0.995 and 39 values at equal intervals between 0.025 and 0.975) were chosen for which the corresponding LG and z-score values were calculated. Note that the LG values depend on the sample size (Number of observations); therefore, the scaling parameter for LG and z-score conversion must be calculated in relation to sample size.
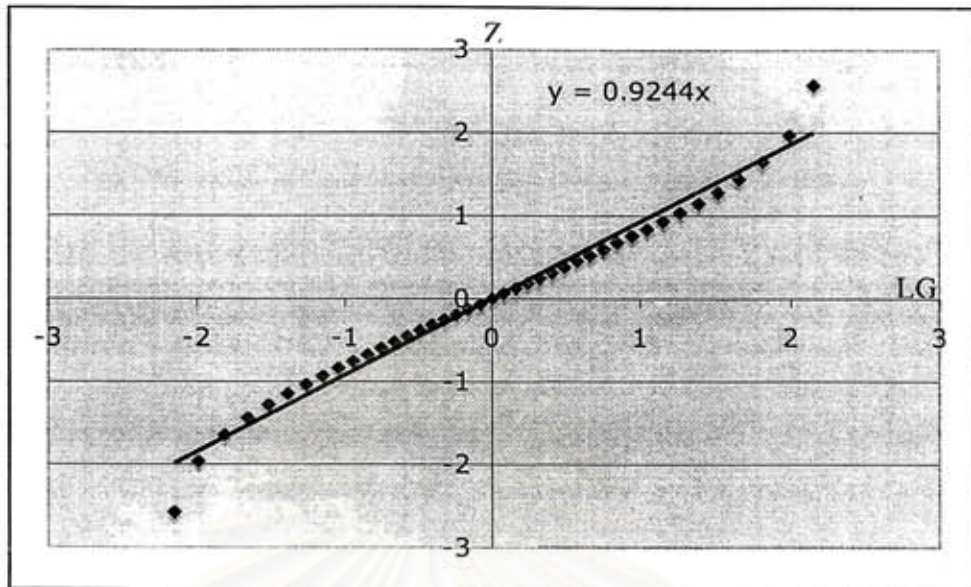
Fig. B1 Relationship between Z scores and LG functions.

Raw data

Observer	1	2	3	4
A	4	2	3	6
B	6	4	5	4
C	1	5	2	4

N = number of observers = 4

m = number of categories = 7

n = number of images = 3

Frequency matrix (F)

Category	1	2	3	4	5	6	7
A	0	1	1	1	0	1	0
B	0	0	0	2	1	1	0
C	1	1	0	1	1	0	0

Cumulative Frequency Matrix (CF)

$$CF_m = \sum_{m=1}^{m} F_m$$

$$= 0 + 1 + 1 + 1 + 0$$

Category	1	2	3	4	5	6
A	0	1	2	3	3	4
B	0	0	0	2	3	4
C	1	2	2	3	4	4

Cumulative Proportion Matrix (CP)

$$CP = \frac{CF}{N}$$

$$= \frac{4}{4}$$

Category	1	2	3	4	5	6
A	0	0.25	0.5	0.75	0.75	1
B	0	0	0	0.5	0.75	1
C	0.25	0.5	0.5	0.75	1	1

Logistic Function Matrix (LG)

$$LG = LN(\frac{(CPN + 0.5)}{(N - CPN + 0.5)})$$

$$= LN(\frac{(1x4 + 0.5)}{(4 - 1x4 + 0.5)})$$

Category	1	2	3	4	5	6
A	-2.197	-0.847	0.000	0.847	0.847	2.197
B	-2.197	-2.197	-2.197	0.000	0.847	2.197
C	-0.847	0.000	0.000	0.847	2.197	2.197

Z-score Matrix (Z)

$$Z = LGx0.9244$$
$$= 2.197x0.9244$$

Category	1	2	3	4	5	6
A	-2.030	-0.783	0.000	0.783	0.783	2.030
B	-2.030	-2.030	-2.030	0.000	0.783	2.030
C	-0.783	0.000	0.000	0.783	2.030	2.030

Difference Matrix (DM)

$$DM_m = Z_{m+1} - Z_m$$
$$= 2.030 - 0.783$$

Category	1	2	3	4	5
A	1.247	0.783	0.783	0.000	1.247
B	0.000	0.000	2.030	0.783	1.247
C	0.783	0.000	0.783	1.247	0

Category	1	2	3	4	5
Mean (D)	0.677	0.261	1.199	0.677	0.832

Category Boundary Estimates (T)

$$T_1 = 0$$
$$T_m = D_{m-1} + T_{m-1}$$
$$= 0.832x2.813$$

Category	1	2	3	4	5	6	7
boundary	0	0.677	0.938	2.136	2.813	3.645	

Scale Values (S)

$$S = T - Z$$
$$= 3.645 - 2.030$$

Category	1	2	3	4	5	6	Mean	Category
A	2.030	1.460	0.938	1.353	2.030	1.615	1.571	4
B	2.030	2.707	2.968	2.136	2.030	1.615	2.248	5
C	0.783	0.677	0.938	1.353	0.783	1.615	1.025	4

95% confident interval

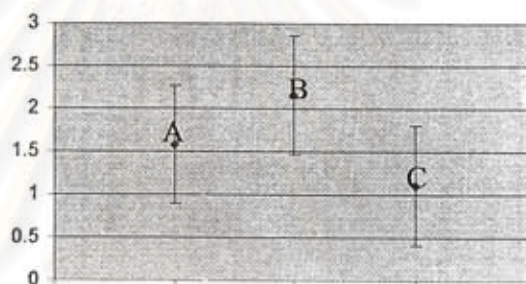$$95\%CL = 1.96\left(\frac{1}{\sqrt{2}}\right)/\sqrt{N}$$
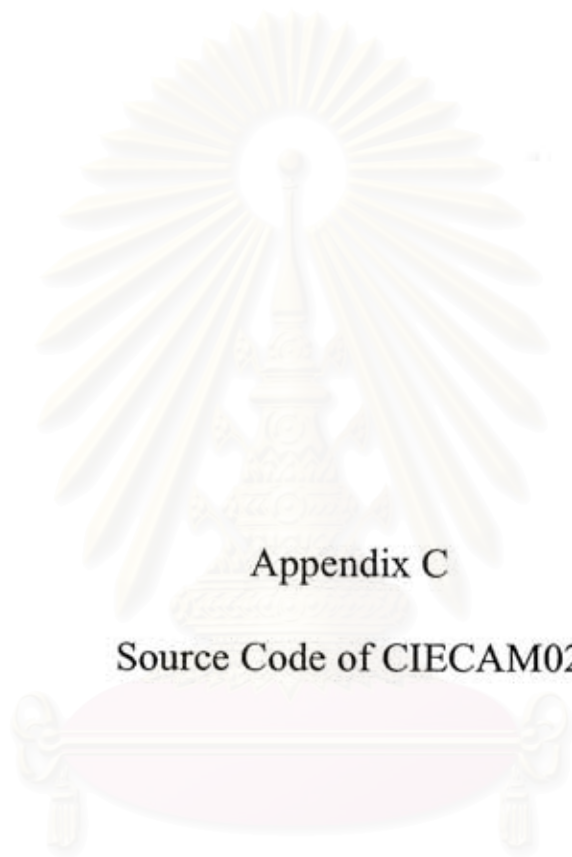$$= 0.693$$

Fig. C-2 Color-match scores from category judgment method for Images A, B, and C.

Appendix C

Source Code of CIECAM02

------------------------Functions of The Calculation------------------

Calculate GOG

```
function [data] = CalGOG(flare,xyzMax,XYZ);

drgb = [0 32 64 96 128 160 192 224 255];
RGB = inv(xyzMax)*XYZ;
R = RGB(1,:)/max(RGB(1,:));
G = RGB(2,:)/max(RGB(2,:));
B = RGB(3,:)/max(RGB(3,:));
maxRGB = [max(RGB(1,:));max(RGB(2,:));max(RGB(3,:))];

%Calculate constance%
SumDelta1 = 100;
for i = 0:300
  Gm = 1+i*0.01;
  for j = 0:100
   Kg = j*0.01;
   Ko = 1-Kg;
     for k = 1:9
        result(k) = (Kg*(drgb(k)/255)+Ko)^Gm;
        if result(k)<=1
           delta(k) = abs(result(k)-R(k));
        else
           delta(k) = 100;
        end;
     end;
     SumDelta2 = sum(delta);
     if SumDelta2 < SumDelta1
        GammaR = Gm;
        GainR = Kg;
        OffsetR = Ko;
        SumDelta1 = SumDelta2;
     end;
  end;
end;

SumDelta1 = 100;
for i = 0:300
  Gm = 1+i*0.01;
  for j = 0:100
   Kg = j*0.01;
   Ko = 1-Kg;
     for k = 1:9
        result(k) = (Kg*(drgb(k)/255)+Ko)^Gm;
        if result(k)<=1
           delta(k) = abs(result(k)-G(k));
```

```
        else
            delta(k) = 100;
        end;
    end;
    SumDelta2 = sum(delta);
    if SumDelta2 < SumDelta1
        GammaG = Gm;
        GainG = Kg;
        OffsetG = Ko;

        SumDelta1 = SumDelta2;
    end;
  end;
end;

SumDelta1 = 100;
for i = 0:300
  Gm = 1+i*0.01;
  for j = 0:100
    Kg = j*0.01;
    Ko = 1-Kg;
      for k = 1:9
        result(k) = (Kg*(drgb(k)/255)+Ko)^Gm;
        if result(k)<=1
            delta(k) = abs(result(k)-B(k));
        else
            delta(k) = 100;
        end;
    end;
    SumDelta2 = sum(delta);
    if SumDelta2 < SumDelta1
        GammaB = Gm;
        GainB = Kg;
        OffsetB = Ko;
        SumDelta1 = SumDelta2;
    end;
  end;
end;
data = [GammaR GammaG GammaB;
        GainR GainG GainB;
        OffsetR OffsetG OffsetB;
        maxRGB(1) maxRGB(2) maxRGB(3);
        flare(1) flare(2) flare(3)];
```

GOG Forward Model
```
function [data] = GOGmodel(dR,kg,gamma);
```

```
[m,n]=size(dR);
ko=1-kg;
for i=1:m
        for j=1:n
                data(i,j) = (kg*(dR(i,j)/255)+ko)^gamma;
        end;
end;
```

GOG Inverse Model

```
function [data] = InvGOGmodel(R,kg,gamma);

[m,n]=size(R);
ko=1-kg;
InvGamma=1/gamma;
for i=1:m
        for j=1:n
                if R(i,j)<= 0;
                        data(i,j) = 0;
                else;
                        data(i,j) = uint8(((((R(i,j)^InvGamma)-ko)/kg)*255);
                end;
        end;
end;
```

CIECAM02 Forward Model (XYZ data > JCh data)

```
function [data] = CIECAM02Fwd(xyz,xyzW,La,Yb,surrounds);

%step 1 Chromatic transform
Yw=xyzW(2);

        %surround
        if surrounds==1 %average
         F = 1;
         c = 0.69;
         Nc = 1;

        elseif surrounds==2 %dim
         F = 0.9;
         c = 0.59;
         Nc = 0.95;

        elseif surrounds==3 %dark
         F = 0.8;
         c = 0.525;
         Nc = 0.8;
```

```
        end;

k = 1/((5*La)+1);
D = F*(1-(1/3.6)*exp(((-1*La)-42)/92));
FL = (0.2*(k^4))*(5*La)+0.1*((1-k^4)^2)*((5*La)^(1/3));
n = Yb/Yw;
Ncb = 0.725*((1/n)^0.2);
Nbb = Ncb;
z = 1.48+(n^0.5);

%Mcat metrix
Mcat = [0.7328 0.4296 -0.1624; -0.7036 1.6975 0.0061; 0.0030 0.0136 0.9834];

rgbW = Mcat*xyzW;
rgb = Mcat*xyz;
Rw = rgbW(1);
Gw = rgbW(2);
Bw = rgbW(3);

r = rgb(1);
g = rgb(2);
b = rgb(3);

%calculate RGBc
Rc = ((D*(Yw/Rw))+(1-D))*r;
Gc = ((D*(Yw/Gw))+(1-D))*g;
Bc = ((D*(Yw/Bw))+(1-D))*b;

Rwc = ((D*(Yw/Rw))+(1-D))*Rw;
Gwc = ((D*(Yw/Gw))+(1-D))*Gw;
Bwc = ((D*(Yw/Bw))+(1-D))*Bw;

rgbc = [Rc; Gc; Bc];
rgbWc = [Rwc; Gwc; Bwc];

%calculate RGB'
MH = [0.38971 0.68898 -0.07868;
      -0.22981 1.18340 0.04641;
      0.00000 0.00000 1.00000];

rgb2 = MH*inv(Mcat)*rgbc;
rgbW2 = MH*inv(Mcat)*rgbWc;

r2 = rgb2(1);
g2 = rgb2(2);
```

```
b2 = rgb2(3);

rW2 = rgbW2(1);
gW2 = rgbW2(2);
bW2 = rgbW2(3);

%calculate RGBa
ra = ((400*(FL*r2/100)^0.42)/(27.13+((FL*r2/100)^0.42)))+0.1;
ga = ((400*(FL*g2/100)^0.42)/(27.13+((FL*g2/100)^0.42)))+0.1;
ba = ((400*(FL*b2/100)^0.42)/(27.13+((FL*b2/100)^0.42)))+0.1;

rWa = ((400*(FL*rW2/100)^0.42)/(27.13+((FL*rW2/100)^0.42)))+0.1;
gWa = ((400*(FL*gW2/100)^0.42)/(27.13+((FL*gW2/100)^0.42)))+0.1;
bWa = ((400*(FL*bW2/100)^0.42)/(27.13+((FL*bW2/100)^0.42)))+0.1;

%step 2 Perceptual
a = ra-(12*ga/11)+(ba/11);
b = (1/9)*(ra+ga-(2*ba));

%calculate Hue
if a==0 && b==0
   h = 0;
elseif b<=0
   h = 360+((360/(2*pi))*atan2(b,a));
else
   h = 360/(2*pi)*atan2(b,a);
end;

e = ((12500/13)*Nc*Ncb)*(cos(h*(pi/180)+2)+3.8);

A = (2*ra+ga+(1/20)*ba-0.305)*Nbb;
Aw = (2*rWa+gWa+(1/20)*bWa-0.305)*Nbb;

J = 100*(A/Aw)^(c*z);
t = (e*((a^2)+(b^2))^0.5)/(ra+ga+((21/20)*ba));
C = (t^0.9)*((J/100)^0.5)*((1.64-(0.29^n))^0.73);

data = [J; C; h;];
```

CIECAM02 Inverse Model (JCh data > XYZ data)
```
function [data] = CIECAM02Inv(JCh,xyzW,La,Yb,surrounds);

J=JCh(1);
C=JCh(2);
h=JCh(3);
```

```
%surround
    if surrounds==1 %average
       F = 1;
       c = 0.69;
       Nc = 1;

    elseif surrounds==2 %dim
       F = 0.9;
       c = 0.59;
       Nc = 0.95;

    elseif surrounds==3 %dark
       F = 0.8;
       c = 0.525;
       Nc = 0.8;

    end;

k = 1/((5*La)+1);
D = F*(1-(1/3.6)*exp(((-1*La)-42)/92));
FL = (0.2*(k^4))*(5*La)+0.1*((1-k^4)^2)*((5*La)^(1/3));

Yw=xyzW(2);
H=(2*pi/360)*h;

n = Yb/Yw;
Ncb = 0.725*((1/n)^0.2);
Nbb = Ncb;
z = 1.48+(n^0.5);

%Mcat metrix
Mcat = [0.7328 0.4296 -0.1624;
        -0.7036 1.6975 0.0061;
        0.0030 0.0136 0.9834];
rgbW = Mcat*xyzW;

Rw = rgbW(1);
Gw = rgbW(2);
Bw = rgbW(3);

Rwc = ((D*(Yw/Rw))+(1-D))*Rw;
Gwc = ((D*(Yw/Gw))+(1-D))*Gw;
Bwc = ((D*(Yw/Bw))+(1-D))*Bw;

rgbWc = [Rwc; Gwc; Bwc];
```

```
%calculate RGBw'
MH = [0.38971 0.68898 -0.07868;
      -0.22981 1.18340 0.04641;
      0.00000 0.00000 1.00000];

rgbW2 = MH*inv(Mcat)*rgbWc;

rW2 = rgbW2(1);
gW2 = rgbW2(2);
bW2 = rgbW2(3);

rWa = ((400*(FL*rW2/100)^0.42)/(27.13+((FL*rW2/100)^0.42)))+0.1;
gWa = ((400*(FL*gW2/100)^0.42)/(27.13+((FL*gW2/100)^0.42)))+0.1;
bWa = ((400*(FL*bW2/100)^0.42)/(27.13+((FL*bW2/100)^0.42)))+0.1;

Aw = (2*rWa+gWa+(1/20)*bWa-0.305)*Nbb;
A = Aw*((J/100)^(1/(c*z)));
e = ((12500/13)*Nc*Ncb)*(cos(h*(pi/180)+2)+3.8);
t = (C/(((J/100)^0.5)*(1.64-(0.29^n))^0.73))^(1/ 0.9);

if t==0
       a = 0;
       b = 0;

elseif abs(sin(h*pi/180)) >= abs(cos(h*pi/180))
a =
(((A/Nbb)+0.305)*(2+(21/20))*(460/1403))/(((e/t)/sin(h*pi/180))+(2+(21/20))
*(220/1403)*(cos(h*pi/180)/sin(h*pi/180))-
(27/1403)+(21/20)*(6300/1403))*(cos(h*pi/180)/sin(h*pi/180));
b =
(((A/Nbb)+0.305)*(2+(21/20))*(460/1403))/(((e/t)/sin(h*pi/180))+(2+(21/20))
*(220/1403)*(cos(h*pi/180)/sin(h*pi/180))-(27/1403)+(21/20)*(6300/1403));

else
a =
(((A/Nbb)+0.305)*(2+(21/20))*(460/1403))/(((e/t)/cos(h*pi/180))+(2+(21/20))
*(220/1403)-((27/1403)-(21/20)*(6300/1403))*(sin(h*pi/180)/cos(h*pi/180)));
b =
(((A/Nbb)+0.305)*(2+(21/20))*(460/1403))/(((e/t)/cos(h*pi/180))+((2+(21/20)
)*(220/1403))-((27/1403)-
(21/20)*(6300/1403))*(sin(h*pi/180)/cos(h*pi/180)))*sin(h*pi/180)/cos(h*pi/1
80);

end;

% Calculate non-linear response
```

```
Ra = (460/1403)*((A/Nbb)+0.305)+(451/1403)*a+(288/1403)*b;
Ga = (460/1403)*((A/Nbb)+0.305)-(891/1403)*a-(261/1403)*b;
Ba = (460/1403)*((A/Nbb)+0.305)-(220/1403)*a-(6300/1403)*b;

R2 = (27.13*(Ra-0.1)/(400.1-Ra))^(1/0.42)*100/FL;
G2 = (27.13*(Ga-0.1)/(400.1-Ga))^(1/0.42)*100/FL;
B2 = (27.13*(Ba-0.1)/(400.1-Ba))^(1/0.42)*100/FL;

RGB2 = [R2; G2; B2];
RGBc = (Mcat*inv(MH))*RGB2;

r = RGBc(1)/((D*(Yw/Rw))+(1-D));
g = RGBc(2)/((D*(Yw/Gw))+(1-D));
b = RGBc(3)/((D*(Yw/Bw))+(1-D));

rgb = [r; g; b];
xyz = inv(Mcat)*rgb;

data=[xyz(1); xyz(2); xyz(3)];
```

CIECAM02

```
function [data] =
CIECAM02(PicXYZ,RefWhite1,RefWhite2,La1,Yb1,La2,Yb2,surrounds);
[m,n,o]=size(PicXYZ);

%forward model
for i=1:m
    for j=1:n
        Pixel = [PicXYZ(i,j,1); PicXYZ(i,j,2); PicXYZ(i,j,3)];
        JCh =
CIECAM02Fwd(double(Pixel),double(RefWhite1),La1,Yb1,surrounds);

        J(i,j)=JCh(1);
        C(i,j)=JCh(2);
        h(i,j)=JCh(3);
    end;
end;

%inverse model
for i=1:m
    for j=1:n
        JCh = [J(i,j);
        C(i,j);
        h(i,j)];
        xyz =
CIECAM02Inv(double(JCh),double(RefWhite2),La2,Yb2,surrounds);
```

```
        data(i,j,1)=xyz(1);
        data(i,j,2)=xyz(2);
        data(i,j,3)=xyz(3);


    end;
end;
```

RGBtoXYZ

```
function [data] = RGBtoXYZ(xyzMax,RGB,GOG)
rgbMax = [GOG(4,1) GOG(4,2)   GOG(4,3)];
flare = [GOG(5,1); GOG(5,2); GOG(5,3)];
[m,n,o]=size(RGB);
   for i=1:m
     for j=1:n
        pixel = [RGB(i,j,1); RGB(i,j,2); RGB(i,j,3)];
        r = GOGmodel(double(pixel(1)),GOG(2,1),GOG(1,1));
        g = GOGmodel(double(pixel(2)),GOG(2,2),GOG(1,2));
        b = GOGmodel(double(pixel(3)),GOG(2,3),GOG(1,3));

        R = r*rgbMax(1);
        G = g*rgbMax(2);
        B = b*rgbMax(3);

        rgb = [R; G; B];
        xyz = flare + xyzMax*rgb;

        data(i,j,1) = xyz(1);
        data(i,j,2) = xyz(2);
        data(i,j,3) = xyz(3);

     end;
   end;
```

XYZtoRGB

```
function [data1,data2] = XYZtoRGB(xyzMax,XYZ,GOG);
rgbMax = [GOG(4,1)  GOG(4,2)  GOG(4,3)];
flare = [GOG(5,1); GOG(5,2); GOG(5,3)];
[m,n,o]=size(XYZ);
for i=1:m
   for j=1:n
   pixel = [XYZ(i,j,1); XYZ(i,j,2); XYZ(i,j,3)];
   pixel2 = pixel-flare;
   RGB = inv(xyzMax)*(pixel2);
   R(i,j) = RGB(1)/rgbMax(1);
   G(i,j) = RGB(2)/rgbMax(2);
```

```
   B(i,j) = RGB(3)/rgbMax(3);

   if R(i,j)>1
      Err(i,j,1) = uint8(255);
   elseif R(i,j)<0
      Err(i,j,1) = uint8(0);
   else
      Err(i,j,1) = uint8(128);
   end;
   if G(i,j)>1
      Err(i,j,2) = uint8(255);
   elseif G(i,j)<0
      Err(i,j,2) = uint8(0);
   else
      Err(i,j,2) = uint8(128);
   end;
   if B(i,j)>1
      Err(i,j,3) = uint8(255);
   elseif B(i,j)<0
      Err(i,j,3) = uint8(0);
   else
      Err(i,j,3) = uint8(128);
   end;
   end;
end;

dr = invGOGmodel(R,GOG(2,1),GOG(1,1));
dg = invGOGmodel(G,GOG(2,2),GOG(1,2));
db = invGOGmodel(B,GOG(2,3),GOG(1,3));

data1(:,:,1)=dr;
data1(:,:,2)=dg;
data1(:,:,3)=db;
data2 = Err;
```

White Patch
```
function [data] = WP_rgb(xyzMax,X,GOG);
%X = PictureRGB
WhiteRGB = max(max(X));
r = WhiteRGB(1);
g = WhiteRGB(2);
b = WhiteRGB(3);

WhitePoint = RGBtoXYZ_point(xyzMax,WhiteRGB,GOG);
data = [WhitePoint(1); WhitePoint(2); WhitePoint(3)];
```

Gray World

```
function [data] = GWrgb(xyzMax,X,GOG);
%X = PictureRGB
MeanRGB = mean(mean(X));
r = MeanRGB(1);
g = MeanRGB(2);
b = MeanRGB(3);
MeanXYZ = RGBtoXYZ_point(xyzMax,MeanRGB,GOG);
x = MeanXYZ(1)/sum(MeanXYZ);
y = MeanXYZ(2)/sum(MeanXYZ);
X = x*100/y;
Z = (1-x-y)*100/y;
data = [X; 100; Z];
```

CIEtest

```
function [data1,data2] =
CIEtest(xyzMax,filename,RefWhite,La,Yb,RefWhite2,GOG);

Picture = imread(filename);
PicXYZ1 = RGBtoXYZ(xyzMax,Picture,GOG);

%%% Calculate Reference White %%%
%White patch RGB
        WpRGB = WP_rgb(xyzMax,Picture,GOG);

%%%%%D65
        D65 = [95.047; 100; 108.88];

%Grey world RGB
        GwRGB = GWrgb(xyzMax,Picture,GOG);

%Monitor
        Monitor = [255; 255; 255];
        Monitor = RGBtoXYZ_point(xyzMax,Monitor,GOG);

%% fix Output condition %%
if RefWhite2 ==1
        Ref2 = [100; 100; 100];
elseif RefWhite2 ==2
        Ref2 = [95.05; 100; 108.88]; %%%D65
elseif RefWhite2 ==3
        Ref2 = [96.42; 100; 82.49]; %%%D50
end;

Yb2 = 20;
```

```
if RefWhite ==1
        Ref1 = WpRGB;
elseif RefWhite ==2
        Ref1 = GwRGB;
elseif RefWhite ==3
        Ref1 = Monitor;
elseif RefWhite ==4
        Ref1 = D65;
end;

if La1==0
        La1 = mean(mean(PicXYZ1(:,:,2)));
else
        La1=La;
end;

if Yb ==0
        Yb1 = 20;
else
        Yb1 = Yb;
end;
PicXYZ2 = CIECAM02(PicXYZ1,Ref1,Ref2,La1,Yb1,La1,Yb1,2);
[data1,data2] = XYZtoRGB(xyzMax,PicXYZ2,GOG);
```

-----------------------Sample of The Calculation------------------

```
%xyzMax is the tristimulus value of Rmax Gmax and Bmax of the monitor
% xyzMax = [Xr Xg Xb;
%            Yr Yg Yb;
%            Zr Zg Zb];

xyzMax = [50.63291139    32.03505355 13.14508277;

         27.45861733  65.53067186 6.523855891;

         4.381694255 10.51606621 69.03602726];

%XYZ is the tristimulus value of Grey scale (drgb)
%XYZ = [X...;
%        Y...;
%        Z...];
XYZ = [0 1.265822785    5.258033106 12.3661149   22.78481013
       36.51411879 53.75851996 73.70983447 96.59201558;
```

```
   0 1.265822785 5.35540409   13.04771178 23.56377799 37.68257059
     55.3067186   76.24148004 99.90262902;

   0 1.071080818 4.381694255 10.51606621 19.47419669 31.1587147
     46.05647517 63.68062317 83.93378773];
```

flare = [0.097370983; 0.097370983; 0.097370983];

%%Finding Gain Offset Gamma%%
GOG = CalGOG(flare,xyzMax,XYZ);

%%[PicRGB,Err] = CIEtest(xyzMax,'A1.tif',RefWhite,La1,Yb1,GOG);

[PicRGB,Err] = CIEtest(xyzMax,'A_1.tif',1,0,0,1,GOG);
imwrite(PicRGB(:,:,:),'A_1WPtoSE.tif'); imwrite(Err(:,:,:),'OutA_1WPtoSe.tif');

VITA

Mr. Mati Bunterm was born on August 21, 1982 in Khonkaen, Thailand. He received his Bachelor's Degree of Science, Photographic Science and Printing Technology program, Faculty of Science, Chulalongkorn University in 2002 and he has been a graduate student in the Imaging Technology Program, Graduate School, Chulalongkorn University since 2003.